QATAR UNIVERSITY

COLLEGE OF ARTS AND SCIENCES

# POLYMER-MATRIX NANOCOMPOSITE MEMBRANES FOR WATER TREATMENT

BY

ABDOLALI MOGHADDASI

A Thesis Submitted to the Faculty of

the College of Arts and Sciences

in Partial Fulfillment

of the Requirements

for the Degree of

Masters of Science in

Material Science and Technology

January 2019

# COMMITTEE PAGE

The members of the Committee approve the Thesis of AbdolAli Moghaddasi defended on [09/12/2018].

_____

Dr. Igor Krupa
Thesis/Dissertation Supervisor

_____

Dr. Khaled A. Mahmoud
Committee Member

_____

Dr. Mohamed Korany Ibrahim Hassan
Committee Member

_____

Dr. Mohammad A. Salim Alghouti
Committee Member

_____

Dr. Adrian Stephanus Luyt
Committee Member

Approved:

_____

Rashid Al-Kuwari, Dean, College of College of Arts and Sciences

# ABSTRACT

MOGHADDASI, ABDOLALI, M., Masters of Science: December : 2018,

Materials Sciences and Technology

Title: Polymer-matrix nanocomposite membranes for water treatment

Supervisor of Thesis: Igor Krupa.

A new generation of advanced fibrous materials with high surface area, large number of pores, high flexibility and adjustable wettability were manufactured from different materials which are viable for many applications related to environment especially oil water separation.

This thesis is focused on the preparation and characterization of two new different polymeric systems applicable in water/oil separation and oil impurities detection. The material system for sensor development is based on styrene isoprene styrene (SIS) elastomer filled with multiwalled carbon nanotubes and system for water/oil separation is composed by co-polyamide (coPA) electrospun mat covered by MXene sheets.

Preparation of composites based on styrene isoprene styrene block polymer (SIS) modified by carbon nanotubes (CNTs) involves optimization of the component ratio and processing conditions utilizing electrospinning method. SIS has ability to absorb oil due to its oleophilic behavior and CNTs enhance the electrical conductivity of composite. The principle of oil sensing is based on the changes of electrical conductivity because of volumetric changes of material due to oil absorption.

Separation of oil from water is performed using membrane technology. We prepared coPA mats via optimization of the polymer solvent/ratio conditions using electrospinning technique. MXene nanoplatelets were prepared from commercial MAX phase by strong etching with HF and delamination.

CoPA mats covered by MXene nanoparticles and this bilayer system was used for water/oil separation. The separation efficiency up to 99.5% which indicates that it is valuable material for separation oil from water.

# DEDICATION

I dedicate my thesis work to my family. A special feeling of gratitude to my loving parents; ***Khadijah*** and ***Mohammad Kazem*** and my lovely children; ***Mohamad*** and ***Hadeel*** for the infinite love and support.

*Most importantly…*

"To my dear wife '***Majedeh'*** for being the shining star in my life."

# ACKNOWLEDGMENTS

I would like to express my special thanks of gratitude to my supervisor, Dr. Igor Krupa who gave me this opportunity to do this work and writing this thesis. All that I have done is only due to such supervision and assistance and I would not forget to thank them.

I would like to express my deepest appreciation to Dr. Patrik Sobolciak. I am extremely thankful to him for providing such a nice support and guidance, although he had busy schedule managing the corporate affairs.

I am thankful to my thesis committee members: Dr. Khaled A. Mahmoud, Dr. Mohammad Korany Hassan, Dr. Mohammad Salem Alghouti and Dr. Adrian Stephanus Luyt for their fruitful comments and productive feedback at all times.

I would like to express my deepest appreciation to department of Materials sciences and Technology, especially Dr. Talal Altahtamouni, Dr. Khalid Yousef and Dr. Ahmed El-Zatahri for their big effort support and encouragement, really their lectures were so interesting, and I have learnt many new things from attending their classes.

I would also like to thank Dr. Anton Popelka for his help and support.

Warmest thanks also go to the Center for Advanced Materials, at Qatar University, for allowing me to conduct research using high-technological laboratory facilities.

Furthermore, I would also like to acknowledge with much appreciation the Central Laboratory Unit (CLU) at Qatar University for testing my samples in their labs specially Mr. Essam Atia and Mr. Mohammad Yousuf.

I am wholeheartedly grateful to all the people I have met during my master's journey; whom have contributed to the development of this work directly and indirectly.

TABLE OF CONTENT

# LIST OF TABLES

# LIST OF FIGURES

# LIST OF ABBREVIATIONS

| | |
|---|---|
| CA | Cellulose acetate |
| CNTs | Carbon nanotubes |
| coPA | Co-polyamide |
| CPCs | Conductive polymer composites |
| DMF | Dimethyl formamide |
| DOWS | Down-hole oil water separation |
| ES | Electrospinning |
| FL | Few layered |
| MEMS | Microelectromechanical |
| MF | Microfiltration |
| ML | Multi layered |
| MWCNT | Multi wall carbon nanotubes |
| MXene | 2D metal carbide |
| NEMS | Nanoelectromechanical |
| NF | Nanofiltration |
| OCA | Oil contact angle |
| PA | Polyamide |

| | |
|---|---|
| PAA | Poly acrylamide |
| PAN | Polyacrylonitrile |
| PDEAEMA | Poly(N,N-diethylaminoethyl methacrylate) |
| PMMA-b-P4VP | Poly(methyl methacrylate-block-poly(4-vinylpyridne) |
| PP | Polypropylene |
| PSO | Polysulfone |
| PVA | Polyvinyl alcohol |
| PVDF | Polyvinylidene fluoride |
| RC | Regenerated cellulose |
| RO | Reverse osmosis |
| SIS | Styrene isoprene styrene block polymer |
| SWCNT | Single wall carbon nanotubes |
| THF | Tetra hydro furan |
| UF | Ultrafine filtration |

# CHAPTER 1: INTRODUCTION

## 1.1 General Background

One of the most important fields that allocated many researcher efforts from long time is water purification and treatment. The health and safety of water in different regions that facing lack of water like arid and semi-arid areas is vital, so more research and studies needed to make the limited sources of water healthy and in good condition for human uses. These studies are very important for recovery, recycling and reusing of water. Treatment of alternative sources of like seawater, river water and wastewater met huge number of researches. Qatar also connected to the sea from several directions and most of oil companies and large industries are often set up along the coast and because of the large transportation of industrial and commercial ships, there is a high probability of pollution of the seawater. On the other hand, because the only way to provide fresh water is seawater and a significant amount of contamination is due to oil and petrochemicals, therefore, it is important to find methods help us to recognize the presence of oily materials and to separate them from water. In regard to tackle issues related to water/oil separation we proposed and prepared sensors and membrane, which can detect oil in water and separate it in the next step.

In this thesis polymeric material, namely styrene isoprene styrene (SIS) copolymer mixed with carbon nanotube (was used as a material which can be potentially applied as the oil sensor. The second investigated system is based on the co-polyamide mat prepared by electrospinning and coated by MXene layers.

Electrospinning is a very useful method used in preparation of membranes and mats from various polymers and their composites with size of nanofibers around few tens

nanometers. The composite combine properties of both components. [1]–[3]. Recently, many polymer nanocomposites reinforced by CNT's, MXenes, graphene etc. were prepared using electrospinning technique. Electrical, mechanical and thermal properties of polymeric matrices are significantly improved through mixing with nanocarbon structures such are CNT's and graphene and final materials are suitable for various applications including sensors, membranes for water treatment etc. [4], [5].

Polymer membranes showed high efficiency in separation oil from water and economically are cheaper that inorganic membranes [6]. Nevertheless, accumulation of particulates inside the pores have negative effect on separation process [7], [8]. Most of membranes for microfiltration (MF) and ultrafiltration (UF) are prepared using polysulfone (PSO) [9], cellulose acetate (CA) [10], polyacrylonitrile (PAN), polyvinylidene fluoride (PVDF) [11], [12] and polyamide (PA). However, polymeric membranes have fouling tendency their surfaces experienced many modifications that enhance antifouling and increase their hydrophilicity.

## 1.2 Objectives

This work focuses on preparation and characterization of two new different polymeric systems. The first one would be potentially applicable for development of sensors detecting various types of oil in water and the second one is convenient for water/oil separation. System for sensor development is based on styrene isoprene styrene (SIS) elastomer filled with multiwalled carbon nanotubes and system for water/oil separation is composed by co-polyamide (coPA) mat covered by MXene sheets. In more details, the scope of this work is focused on the following activities:

1. Detection of oil in water using electrically conductive polymeric sensors. This work

consists of two parts:

a. Preparation of composites based on SIS modified by carbon nanotubes (CNTs) what involves optimization of the component ratio and processing conditions utilizing electrospinning method. SIS has ability to absorb oil due to its oleophilic behavior and CNTs enhance the electrical conductivity of composite. The principle of oil sensing is based on the changes of electrical conductivity as a consequence of volumetric changes of material due to oil absorption. An excellent dispersion of CNTs is very important in SIS-CNT preparation process.

b. Despite, the fact that SIS is well soluble in various organic, unipolar solvents, the preparation of mats requires careful selection of an appropriate solvent and optimization of processing parameters.

c. Study of electrical properties of prepared composites and characterization of the sensing sensitivity.

2. Separation of oil from water using membrane technology (polymeric membrane) which involves coming parts:

a. Preparation of coPA mate via optimization of the polymer solvent/ ratio conditions using electrospinning technique.

b. Synthesizing of MXene from commercial MAX phase by strong etching with HF and delamination.

c. Fabrication of coPA mats covered by MXene nanoparticles

d. A Study the effect of MXene particles on water/oil separation efficiency.

# CHAPTER 2: LITERATURE REVIEW

In this chapter, a brief overview of oil / water separation techniques in general is provided. Furthermore, of the membrane techniques preparation, particularly membranes used for oil/water separation will be discussed and incorporation of nanosized material specially CNT's and MXene to the structure of nanofiber. The preparation of composites' membranes using electrospinning technique and their applications as sensors and membranes in different field especially oil /water separation will be summarized.

## 2.1 Sensors

Any sensing system consist of three core parts, the sensing element, transducer and the output unit. The energy simulated by input signal and external source of energy needed is considered for classification of sensors as passive and active sensors. The passive sensor operation is based on simulation of energy by input signals without effect of any external source of energy. For example, piezoelectric sensors, which are able to produce electrical charge without influence of any external energy under mechanical stress [13]. More examples of passive sensors are photodiode and thermocouple [14], [15]. Unlike passive sensors, active sensors to simulate energy need signal or extra energy from external energy source. The sensors modify the signal to create an output signal. Strain gauge and heat sensing resistor are examples of active sensors. Strain gouge computes applied load based on change in resistivity and supplied current alternation. Likewise, heat sensing resistor notifies the resistivity without producing any current can be measured to compute the temperature in presence of external signal [16]–[18]. Additionally, sensors are also classified on the base of physical contact between sensing element and the analyte to contact and non-contact sensors. Laser sensor is example of non-contact sensors to measure

the distance while typically, chemicals and gas sensors count as contact sensors which direct physical contact needed between analyte and sensor [14], [19], [20].

### *2.1.1 Conductive Polymeric Composites (CPCs)*

Newly, many researches are conducted the work on conductive polymer composites for liquid and gas sensing. CPCs have low density, they are flexible, and they possess some level of electrical conductivity [21]–[25]. The CPCs resistivity increase once they exposed to organic solvent vapor or liquid due to wetting the CPCs by organic solvent and diffusing into the composite resulting in swelling of polymer matrix, therefore increasing the space between conductive fillers thereby increasing of the resistivity. The resistivity of CPCs will release to its initial value after removing from the solvent vapor due to desorption of the vapor that leads to de-swelling of the polymer matrix and accordingly decrease of the distance between conductive filler and resistivity [26], [27]. In addition to the solubility of the solvent to polymer the sensing functioning depending on thicknesses, the content of conducive filler and the organic vapor saturated pressure [28]–[31]. Typically, for CPCs preparation, solution or melting mixing is used for an incorporation of conductive nanofiller into polymer matrix [32]. Distribution, size and geometrical parameters (e.g. aspect ratio) of nanoparticles are crucial for reaching of percolation threshold, which is known as the critical volume percentage of conductive nanoparticles at transition of polymer from insulator to conductive. From this reason, conductive nanofiller such as CNTs, graphite and carbon black are often preferred as they can form continuous conductive network with a matrix at low concentrations [33]–[37].

### *2.1.2 Application of Sensors*

The sensors development represents important research activity due to the large use

in industry including applications such are electronic devices, agriculture, aviation, biomedical and automation. The classification of sensors is based on their function in detecting signals from the subject that can be used for qualitative and quantitative measurements. The signals can be electrical, chemical, mechanical, radiant, magnetic or thermal [38]–[40]. Among other applications, sensors also have found applicability in oil detection. The principle is the change of some physical or chemical properties in the presence of oil in water. Here are some types of sensor used for detecting the signals comes from physical or chemical changes occurs on species.

### *2.1.3 Classification Sensors:*

Sensors classification is based on the type of response and the application they are used for. Optical sensor response to optical inputs like light velocity, wavelength and frequency [41]. Chemical sensors are based on interaction of the sensing surface with analyte molecules, this interaction could be ion exchange, adsorption and liquid to liquid extraction[42]. Recently developed advanced or smart sensors that surpassed the rest due to utilizing advance material which are more sensitive and accurate in microelectromechanical (MEMS) and nanoelectromechanical (NEMS) system [43], [44].

### *2.1.4 Carbon Nanotubes*

Carbon nanotube were discovered by Iijima in 1991 [42], and strongly influenced advances in polymer nanocomposite field. The first reinforced polymer nanocomposite by carbon nanotube reported by Ajayan et al. [45]. Carbon nanotubes are rolled up of hexagonal structure graphene into cylindrical shape, which caped from sides, by half from of fullerene structure. There are different kinds of CNTs, which are SWCNTs, or single walled carbon nanotubes, which include single shell of graphene and MWCNTs or multi-

walled carbon nanotubes, which have multilayer of graphene sheets. Carbon nanotube based on atomic arrangement can be metallic or semiconducting [46].

In this work, CNTs used due to its excellent electrical conductivity to be insert inside electrospun mat form obtaining electrically conductive polymer, which is able to response to resistivity changes due to volumetric changes.

### *2.1.5 Carbon Nanotubes/Polymer Nanocomposites*

Polymer composites widely used in industrial applications as sensors, electrical insulators, aerospace applications, thermal insulator, automobiles etc. However, there were some limitation for polymer composites therefore due to huge application incorporation of CNTs with excellent properties into the polymer matrix structure as a filler helped in conquering the limitations.

### *2.1.6 Preparation of Carbon Nanotubes/polymer Nanocomposites*

To enhance the properties of CNTs/polymer, homogeneous dispersion of carbon nanotubes is very critical by keeping tough interaction and adhesion between the filler and matrix. Several methods were utilized to optimize performance of dispersibility and interaction. The most common methods are in situ polymerization, solution mixing and melt processing, which are commercially scalable. CNTs can be dispersed well in a specific solvent followed by the polymer dissolving in the mixture. Various methods are utilized for enhancing the dispersion process. Ultrasonic agitation was used by Safadi et al. for MWNTs dispersion into the polystyrene matrix [47], [48]. Some studies represented the modification of CNTs surfaces for better dispersion by introducing functional groups[49]. Addition of surfactants is another approach to tackle the compatibility issues of polymer and fillers [50], [51]. To avoid agglomeration after solvent evaporation, spin casting

showed by Du et al [52]. Electrospinning is another method which has been used for producing polymer nanofibers to get optimum dispersion using electric field [53], [54].

## 2.2 Membrane

### *2.2.1 Oil/water Separation Techniques*

Many techniques and equipment have been reported in literature for separation of oil from water. Oil occurs in water in different types of contaminations involving floating on water, emulsified, suspended solid and dissolved. The most known techniques or separator considered following parameter of oil and water: oil drop size, oil density, viscosity of water, concentration of oil and oil-water flow rate. These techniques utilize: solvent extraction, marine oily water separator, gravity plate separator, API oil–water separator, centrifuge oily water separator, hydro cyclone oily water separator, flotation technique, nutshell filtration technique, electrochemical emulsification, downhole oil–water separation (DOWS), bioremediation technique and membrane technology.

### *2.2.2 Membrane Technology*

Membrane in general is a barrier with pores in different sizes, which permits some small particles, molecules or ions and prevent others with larger size from passing through. Material that is used for membrane synthesizing must be able to form stable thin film. Accordingly, metals, ceramics, polymers, monolayer liquids and glass are proper materials for membranes [55], [56]. Basically, three phenomena are important in membranes preparation, namely the effect of adsorption, electrostatic interactions and molecular sieving [57], [58]. Classification of membrane is mainly based on pore size, and material used for membrane synthetization and membrane structure [59]. According to their structure, they can be classify as dense homogenous asymmetric membranes or porous

membrane [59]. Most of recent membrane are combination of both porous membrane with a film of dense membrane on top [60], [61]. Based on the fabrication, material membranes can be classified as organic, inorganic or hybrid membranes [62]. Polymers are mainly used in manufacturing of industrial membranes [63]. Except polymers, ceramics, metals, elemental carbon or zeolite are utilized used in manufacturing of inorganic membranes [64]. High temperature, pressure resistivity and high stability under severe conditions are properties of inorganic membranes [62], [65].

In comparison to traditional techniques, the oil removal separation processes using membrane are the most suitable. The traditional methods are applicable for immiscible oil/water mixture separation while not efficient for emulsified oil/water mixture particularly not when the drop size is less than 20 μm (surfactant-stabilized microemulsions) therefore more additional treatments are needed [66]. Classification of membranes can be done according to their hydrophobicity/hydrophilicity and oleophobicity/oleophilicity, which is based on their wettability toward water and oil [67]. Generally, the energy-intensive cross-flow filtration system utilizes hydrophobic (or superhydrophobic) and oleophilic membranes. This is not suitable for oil/water separations techniques dependent on gravity because of a formation of a barrier, which blocks permeation of oil. Hydrophobic and oleophilic membranes are fouled readily by oil while de-emulsification process [68]. Classic hydrophilic membranes are more resistant against fouling and powerful for gravity-based de-emulsification [66] but not proper for free oil-water mixture or emulsion of water-in-oil separation, as both water and oil can freely pass through them. These are very considerable technical challenges in process of oil/water separation because the absorption of oil onto surface of membrane jointly with fouling for long term use

will influence the efficiency of separation [69]. Thus, the challenge is developing novel materials, which have large separation capacity, resistance to fouling of oil, and can be easily recycled. **Superhydrophobic/superoleophilic or superhydrophilic/superoleophobic** surfaces promising effective oil/water separation by removing oil from water or vice versa from oil/water mixtures either through absorption or filtration.

*2.2.2.1 Superhydrophilic/superoleophobic Membranes*

Somewhat on the same surface the combination of superhydrophilicity and superoleophobicity is unusual, its refers to surface tension of oil and water which are (~20-60 and ~72 mN/m respectively thus superoleophobic surface can be superhydrophobic [70]. Xue et al. and Tuteja et al. have leading work in this field. They fabricate a membrane that was simultaneously superhydrophilic and superhydrophobic in air and under water [71], [72]. 50 wt.% fluorodecyl POSS + PMMA (poly(methylmethacrylate)) microbeads mixed onto stainless steel wire mesh using electrospinning technique. Prepared membrane was able to remove emulsion oil with diameter larger than 1 μm [72]. Several researches conducted on superhydrophobicity/superhydrophilicity and many papers published [73]–[77]. Krupa et al. worked on zwitterionic based polymer or monolayer or monolayer with high hydrophilicity and molecules with balanced charge, they produced modified membrane owing superhydrophilic/superoleophobic properties. They have drowned up a surface of rough gold from zwitterionic or quaternary ammonium based on monolayer with terminal group of chloride counterion. Superhydrophilic and underwater superoleophobic properties are represented by these modified surfaces, which prevent biofouling by repelling bacteria and cell adhesion. Another example of this type of membranes was created by depositing of $CaCO_3$-based mineral coating on poly(acrylic acid) (PAA)-grafted

PP nanofibrous membranes [78]. Plentiful amount of water trapped in the rigid mineral coating from an aqueous environment resulting in a strong hydrated layer on the surface of membrane pore, therefore supplying underwater superoleophobicity for membrane. The high efficient with high water flux separation of various oil/water mixture and emulsion can be done under pressure or even the effect of gravity [78], [79].

*2.2.2.2 Superhydrophobic/Superoleophilic Membranes*

The superwettable nanofiber membranes are effective in repelling water and lets oil to pass through it easily hence obtaining high efficiency and selectivity [80]. Stating on the Wenzel and Cassie-Baxter model, introducing of an adequate multiscale roughness can make a superhydrophobic from hydrophobic surface, while, superoleophilic from oleophilic surface [81]–[83]. Accordingly, by combination of appropriate rough topography and low surface energy can achieve a membrane surface that shows properties of superhydrophobic and superoleophilic simultaneously [84], [85]. Superhydrophobic and superoleophilic membranes are efficient for separation oil from water even for low concentrations. Superhydrophobic and superoleophilic membranes first reported by Jiang et al. in 2011 was develop by coating still mesh with thin film of hydrogel (polyacrylamide (PAM)) to be used for separation oil from water [74]. The separation efficiency of oil/water mixture was more than 99%. Disadvantages of such material the supporting mesh was owing pores with large size which was not suitable for separation of emulsified oil/water [86]. Polyamide membrane with silica nanoparticles for oil/water separation demonstrated high permeate flux and stability was fabricated by Maad et al. The membrane presented superydrophobicity in the air and superoleophilicity in neutral underwater. A simple method was displayed by Zhang et al. in their work they utilized modified phase-inversion

process for fabrication of superhydrophobic/superoleophilic poly(vinylidene fluoride) (PVDF) membrane [84]. In this process, PVDF was dissolved in N-methyl-2-pyrrolidone and an inert solvent additive such as ammonia water added to solution. Emulsions of both micro- and nanometer-sized surfactant-free and surfactant stabilized was separated by filtration driven only with gravity. The purity of oil in filtrate was more than 99.95 wt.% and flux 1710 L $m^{-2}$ $h^{-1}$.

*2.2.2.3 Nanofibrous Ultrafiltration Membranes*

Recently, electrospun nanofibrous membranes were proposed as good candidates for various kinds of water purification because the show higher permeability and lower cost of energy in comparison than traditional techniques [87], [88]. In order to prevent fouling problems of membranes, membranes surfaces are modified via deposition of a thin layer of hydrophilic materials , like chitosan [89], polyamide [90], or polyvinylalcohol) (PVA) [91], [92], by interfacial polymerization or physical adsorption. For obtaining high flux for separation of oil/water emulsion, modification of nanofibrous ultrafiltration membranes by hydrophilic membrane was performed by Chu et al. [89], [91].

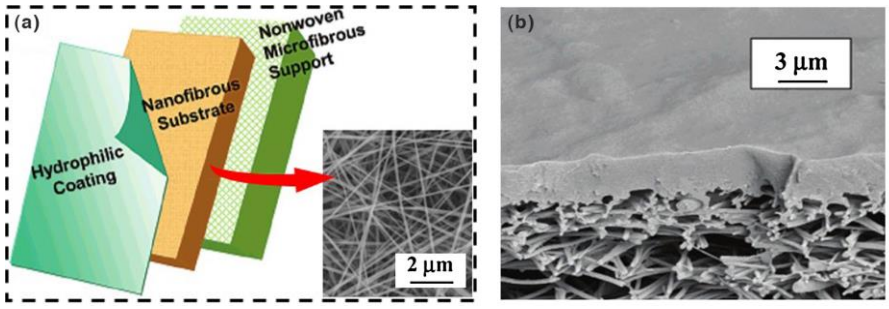


Figure 1 The three-tier approach to the fabrication of high-flux and low-fouling ultrafiltration membranes. (b) Typical top structure of a fractured composite membrane [91].

Figure 1 a and b, representing three layers of high flux and low fouling ultrafiltration membrane which consist of nonwoven microfibrous as a substrate coated with electrospun nanofibrous (PVA, PAN, etc.) then covered with hydrophilic layer such as chitosan or PVA hydrogel. The flux and antifouling properties enhanced significantly for prepared membrane due to its high porosity and smooth, thin layer of barrier [89], [91], [92].

*2.2.2.4 Smart special Wettable Nanofibrous Membranes*

Stimuli-responsive wettability membrane have received an attraction due to their relevance in essential studies and applications in industry [93], [94]. An external accelerator or stimulus must apply to achieve a controllable surface wettability. Several stimuluses were reported like temperature [95], pH [96], [97], electric fields [98], light [99], and gas [100]. The acidic and basic functional groups on polymer structure give the polymer behavior of pH-responsive wetting due to influencing of polymer morphology and charges by various pH solutions. A smart fibrous membrane fabrication was reported by Li and co-workers. Fibers of poly(methyl methacrylate)-block- poly(4-vinylpyridine) (PMMA-b-P4VP) were deposited on mesh of stainless steel using electrospinning method [101]. The fabricated membrane was provided with convertible surface wettability via the PH-responsive P4VP and the PMMA, which has underwater oleophilicity/hydrophilicity properties toward emulsified oil in water. PMMA-co-poly(N,N-diethylaminoethyl methacrylate) (PDEAEMA) nanofibrous membranes were developed recently as $CO_2$-responcive for surface wettability control which represented a switchable oil/water wettability for controllable separation of oil/water emulsion [100]. According to this design a hydrophilic chain extended from the reaction of $CO_2$ with PDEAEMA tertiary amine

groups [102], [103] which can recover its overall hydrophobicity properties when exposed to $N_2$ for removing $CO_2$. Thus, the alternating $CO_2/N_2$ stimulation performs the adjustment of the fabricated nanofibrous membranes oil/water wettability. In addition, $CO_2$-responsiveness together with porous nanostructure empower the membranes to function as oil/water on-off switch. Additionally, smart dual layer nanofibrous membrane is also prepared for oil/water separation that has tendency to oil-transport capacity [104].

### *2.2.3 Classification of Membranes*

Membranes can be classified according their pores size and subsequent ability to rejecting certain size particles. Nanofiltration (NF) membranes have ability of rejecting particles with size less than 0.002 µm. Ultrafine filtration (UF) membranes can remove particles which have size range from 0.005-2 µm and works at pressure range of 10-700 kPa. Microfiltration (MF) membranes operates on removing particles and contamination in size range of 0.08-2 µm and works at pressure range of 7-100 kPa [105].

### *2.2.4 Advantages and Disadvantages of Polymeric Membranes*

Since oily content is hydrophobic and sticking on hydrophobic surfaces, the fouling will reduce by utilizing hydrophilic membranes. Two major methods are used to improve polymeric membranes hydrophilicity, chemical or physical modification of membrane surfaces or via adding hydrophilic material to the polymer structure [7]. However, various parameters influence the membrane functioning even on membranes with modified surface including trans-membrane pressure, temperature, velocity of cross flow and pH. Decreasing the membrane, increasing the efficiency of separation and chemical resistance reinforcing of membrane are necessary for polymeric membrane to be economically and technically useful [106]. Researcher achieved this enhancement using various techniques

of preparation or modification. The hydrophilicity of membrane improved using different methods of chemical or physical such as incorporation of nanoparticles [107], interfacial polymerization [108] and surface grafting. Preparation of polymeric membrane is simple, low cost and operating conditions are moderated. Despite these advantages the main disadvantages of polymeric membranes are the leaching and clustering of the incorporated particles [109].

### *2.2.5 MXenes for Water Treatment*

MXenes are 2D particles prepared by strong etching of three-dimensional MAX phases by removing "A" element from MAX phase, which is mostly from group III A or IV A with keeping the transition metal (titanium) which is indicated by letter "M" and C or N that are denoted as "X" intact. The layer that exfoliated during etching is terminated by functional groups such as OH, F and O signified as T. Recently this new class of materials gain lot of interest in many applications due to high surface area, good mechanical and electrical properties. The 2D interlayer channels as well as high hydrophilicity made possible to use MXene in water desalination. Liu et al. used MXene membrane for pervaporation desalination. They use simple filtration method for fabrication ultrathin 2D MXene for water desalination purpose. The prepared MXene membrane showed excellent performance resulted from high hydrophilicity and transport channels with unique 2D interlayer structure. High water flux was recorded for MXene membrane (85.4/$m^2$h) and rejection of 99.5 % of NaCl [110]. Guo and co-workers modified MXene via Ar Plasma for efficient water desalination. The fabricated membrane exhibited high rate of salt removal and total increasing in removal capacity [111].

### *2.2.6 Commercial Polymeric Membrane Performance*

Commercial polymeric membranes are used widely for various separation purposes. Table is showing comparison of the performance of UF Flat-Sheet membranes utilized for oil/water separation fabricated by different manufacturer based on the polymer used and their flux rate. (Table 1)

### *2.2.7 Recent Polymeric Membrane Used for Water/oil Separation*

Some recently developed polymeric membranes and ceramic membranes with their fabrication/modification methods, additive and component, performance and efficiency are listed in Table 2. Most of polymeric membranes exhibiting high separation efficiency and high flux of dispersion of water.

Table 1. *Comparison of different commercial polymeric membranes based on flux rate [134]*

| **Manufacturer** | **Series** | **Type of membrane** | **Polymer** | **Use** | **Flux $L/m^2h^{-1}/bar$** |
|---|---|---|---|---|---|
| GE Osmonics | MW | Hydrophilic | PAN | Oil/water separation | 4466/1.38 |
| Trisep | UB70 | Hydrophilic | Polyvinylidene Fluoride | Industrial waste water | 1198/0.206 |
| Microdyn Nadir | UC500 | Extremely hydrophilic | RC | Waste water | 7336/2 |

Table 2. *List of latest polymeric membrane fabricated and tested for separation oil/water emulsion [112].*

| Membrane name | Fabrication/modification techniques | Additives/component used | Performance/efficiency | Ref. |
|---|---|---|---|---|
| Zwitterionic PVDF/PSH | Blending/in situ cross-linking/NIPS | PDH | high water flux and 98% flux recovery | [113] |
| PLA/P34HB | Blend electrospinning | PLA | Enhanced water flux | [114] |
| PES | Dry-wet NIPS | SiO2/ZnO | High flux | [115] |
| PVDF | Electrospinning | Silica composite | 2000 $L/m^2h^1$ | [116] |
| PSf | Blending | PVP and PEG | good flux of dispersion | [117] |
| PVDF-$TiO_2$ | Blending | PVP and PEG | 99% rejection of oil | [118] |
| PES/Pluronic membranes F127 | Blending | Pluronic F127 | fine hydrophilicity antifouling property | [119] |
| PSf | Phase inversion | PEG, PVP, PEI and PES | High flux, rejection coefficient is high | [120] |
| PTFE | Deposition/coating | PDA and PEI | Superior hydrophilicity and chemical stability | [121] |
| PMMA-b-PNIPAAm | Solution-casting method and electrospinning | PNIPAAm | Flux rate 9400 $L/m^2h$ | [122] |
| PVDF | Coating | NP of $TiO_2$ | Efficiency 99% | [123] |
| ENF | Cross-linking/Coating | PAN/HPEI/PDA | High oil contact angle (162°) flux 1600 $L/m^2h$ | [124] |
| Stainless steel meshes | Spray coating | NP of WO3 | Separation efficiency 99% | [125] |
| PVDF | Grafting | PVP | Excellent fouling resistance | [126] |
| Cellulose UF | Grafting of PNIPAAm-PPEGMA, ATRP | PNIPAAm- PPEGMA | Oil rejection 97% | [127] |
| PVDF-g-PAA | Polymerization and electrospinning | PAA | super- hydrophilicity | [128] |
| PVDF | Amidation reaction | PEI | high flux with premium fouling resistance | [129] |
| PAN-g-CA | Grafting/free radical | PAN | Improved its hydrophilicity | [130] |
| PVDF | Electrospinning | TEA | Flux >23,000 L/m2h | [131] |
| PVDF/$SiO_2$-PNIPAM | Radical polymerization | PNIPAM | lower oil adsorption mile | [132] |
| PAN | Electrospinning | ZIF-8 | high flux and separation efficiency, OCA=159° | [133] |

# CHAPTER 3: EXPERIMENTAL PROCEDURES

## 3.1 Materials

Styrene isoprene styrene (SIS) Kraton, USA), Toluene (Sigma Aldrich, USA), Dimethyl formamide (DMF) (Sigma Aldrich, USA), Tetrahydrofuran (THF) (Sigma Aldrich, USA), Carbon nanotubes modified by COOH or $NH_2$ group (cheaptubes.com), Co-polyamide 6,10 (VestameltX1010, EVONIK Industries, Germany), n-propanol (Sigma Aldrich, USA), $Ti_3AlC_2$ (Y-Carbon, Ltd., Ukraine), Lithium fluoride (Sigma Aldrich, USA), sunflower vegetable oil (Adams group, USA),

## 3.2 Preparation of SIS-CNT's Sensors

Toluene and tetrahydrofuran/dimethyl formamide mixture were chosen for preparation of SIS sensors to find the optimum concentration for SIS to obtain best mat from electrospinning.

### *3.2.1 Preparation of SIS Solution in Toluene*

First, 1.5 mg CNT-$NH_2$ added to 5.2 ml of toluene and placed for sonication by using inner probe sonicator (to be check every 10 minutes and this step repeated 2 times for 10-15 minutes each time). The same steps were done for CNT-COOH (multiwall) to see it's dispersion in toluene in comparison with multiwalled CNT-$NH_2$ dispersion. Since multiwalled CNT-COOH exhibited better dispersivity compare to CNT-$NH_2$, the work was focused on CNT-COOH.

For better dispersion, 2 drops of triton X (surfactant) added to the solution, and then 0.75 g of SIS added to the mixture and stirred for 20 minutes until whole polymer dissolved completely. The mixture then sonicated by inner probe sonicator machine for 15 minutes.

### *3.2.2 Preparation of SIS Solution Using Mixture DMF and THF*

Solutions of SIS in THF/DMF was prepared according previous paragraph 3.2.1. Various concentration of SIS (from 10 to 15 wt.%) in THF/DMF 50:50 (v/v) and THF/DMF 80:20 (v/v) was prepared. Concentration of CNTs varied from 0.5 to 10 wt.% relative to concentration of polymer.

### *3.2.3 Electrospinning*

Electrospun nanofibers were fabricated by NaBond (Shenzhen, China) electrospinning device. Typically, 5 mL SIS/CNTs dispersions were filled into a 10-mL syringe, with a blunt-end, stainless steel needle type 8. The needle was connected to the emitting electrode of a high-voltage supply capable of generating DC voltages in the range of 0–50 kV. An aluminum foil on the rotation drum collector was used as the collection screen connected to the ground electrode of the power supply with the distance between the screen and the needle tip 15 cm. The electrospinning process was carried out at room temperature at a voltage of 15 kV. The solutions were electrospun continuously for 30 min at a flow rate 1.0 ml/h and drum speed of 200 RPM to obtain sufficient amount of electrospun fibers to be able peel them out from the aluminum support.

### *3.2.4 Fabrication of Sensor*

For sensor fabrication 13 wt.% of SIS have been chosen due to most uniform fiber production. Loading of CNT was from 2 to 10 wt.% related to concentration of SIS. Gold interdigitated electrodes were provided for each sample, then, took to be coated with the fiber under electrospinning. Then electrospinning ran for 20 minutes under 20 KV and 2 ml/hr. flow rate. Layer of SIS-CNTs fiber settled on interdigitated gold electrodes, which placed in oven for 24 hr. and 50 °C.

### *3.2.5 Sensors Absorbance Capacity Measurements*

Square piece of electrospun mat and casted film was immersed in oil for one hour, then removed for measuring their capacity to absorption oil and subsequently retuned back to oil and measurement was repeat after twenty hours. The following equation was used to measure absorbance capacity:

$$\text{Absorbance capacity\%} = (m - m_0)/m_0 \times 100$$

where,

$m_0$ = mass of sample

m = mass of sample + mass of absorbed oil

### *3.2.6 Resistivity Measurements*

In order to examine sensors performance, effect of saturated solvents vapor and oil droplets on sensors resistance were studied.

#### *3.2.6.1 Vapor Sensing Test*

Gold electrodes were coated with 13 wt.% SIS and 10 wt.% of CNT using electrospinning technique. Sensors were exposed to saturated vapor of toluene and the rest to saturated vapor of acetone. Then the electrodes terminals were connected to Source Meter system (KEITHLEY 2635A, USA) under 10 mA to measure the resistivity of samples. The relative resistivity ($A_R$) for each sensor were calculated using the following equation

$$\mathbf{A_R = (R - R_0)/R_0 \times 100\%}$$

- R is the resistance at time t
- $R_0$ is the original resistance of the sample.

#### *3.2.6.2 Oil Sensing Test*

Water, vegetable oil and their mixture with concentration 10, 100 and 1000 ppm of vegetable oil were prepared. Several sensors were prepared by electrospinning of 13 wt.% of SIS and 10 wt.% of CNT on gold electrodes. Then measured the resistivity changes using KEITHLEY 2635A system Source Meter upon exposing to drops of different sample by the time. Relative resistivities were calculated employing previous equation.

## 3.3 Co-polyamide-MXene Membrane Preparation

### *3.3.1 Preparation of MXene from MAXene Phase*

MXene 2D particles were prepared by three steps process, which involves, the etching process, washing and drying process and delamination.

#### *3.3.1.1 Preparing LiF.HCl Etched MXene*

Preparation of $Ti_3C_2$ was done as follow: a thermal couple was placed in oil bath and the temperature was adjusted to 35 °C. 15 ml of water was added to a plastic bottle with a cap and mixed with 15 ml of conc. HCl, followed by 30 minutes temperature stabilization. Then, 1.98 gram of LiF was added to the mixture with continuous stirring for 15 minutes.

Then, three grams of $Ti_3Al_2C_2$ (MAXene) was added steadily to acid solution and kept in oil bath with continuous stirring for 24 hours.

#### *3.3.1.2 Washing and Drying Process*

The mixture was diluted by adding 50 ml of deionized water while stirring for 5 minutes in the oil bath. Then, the mixture was removed from the bath and distributed equally into 50 ml falcon tubes and took for centrifugation at 3500 rpm. for 2 minutes. This step was repeated until appeared green color for supernatant, and pH was about 6. The

supernatant was removed and added ethanol followed by filtration using 0.45 µm cellulose nitrate membrane. The filter paper with wet product was dried overnight at room temperature in plastic petri dish.

*3.3.1.3 Delamination*

For delamination step, 200 ml of deionized water was degassed for 15 minutes using nitrogen gas. 1.2 g of prepared MXene was added to degassed water and place into sonicator bath for 45 minutes. Then, centrifugation at 3500 rpm for 45 minutes was done.

### *3.3.2 Preparation of Co-Polyamide Membrane*

Co-polyamide membrane prepared by electrospinning the 18wt.% of co-polyamide in n-propanol. coPA has high solubility in n-propanol but it was accelerated by heating. After fabrication showed high stability even at room temperature[42].

Electrospun nanofibers were fabricated by NaBond (Shenzhen, China) electrospinning device. Typically, 5 mL coPA/CNC suspensions were filled into a 10-mL syringe, with a blunt-end, stainless steel needle type 8. The needle was connected to the emitting electrode of a high-voltage supply capable of generating DC voltages in the range of 0–50 kV. An aluminum foil on the rotation drum collector was used as the collection screen connected to the ground electrode of the power supply with the distance between the screen and the needle tip 10 cm. The electrospinning process was carried out at room temperature at a voltage of 20 kV. The solutions were electrospun continuously for 30 min at a flow rate 0.5 ml/h and drum speed of 200 RPM in order to obtain sufficient amount of electrospun fibers to be able peel them out from the aluminum support.

### *3.3.3 Fabrication of Co-polyamide Coated by MXene Membrane*

Glass filtration unit technique was used for fabrication of coPA/MXene

membranes. 50 mg of single layer MXene ($Ti_3C_2$) is added to 50 ml of deionized water and sonicated for 20 minutes. Then, suspension was poured onto co-polyamide membrane under vacuum. Subsequently membrane with formed MXene layer on surface was washed with water to remove all unattached MXene particles until obtaining transparent filtrate confirmed by UV spectroscopy.

The similar steps in previous section was applied to prepare ML-MXene/polyamide membrane.

### *3.3.4 Spectroscopy*

Spectra were recorded on Spectrophotometer (Libra biochrom, USA) a Suprasil quartz cuvette (10 mm) from Heraeus Quarzglas GmbH. The data were obtained at a constant bandpass with a resolution of less than 2 nm.

#### *3.3.4.1 Preparation of Different Concentration of Oil Sample*

For testing the membrane efficiency, first prepared oil stock solution 1000 ppm by adding 0.5 gram of vegetable oil in 500 ml of deionized water and sonication for 20 minutes. Then stock solution diluted to 100 and 10 ppm by adding 20 ml of stock solution in 180 ml of deionized water and 180 ml of the stock solution in 20 ml of 1000 ppm neat vegetable oil respectively.

### *3.3.5 Filtration Using Glass Filtration System*

Glass filtration system used for testing the membranes efficiency. The prepared membranes were attached to the system to separate oil from water.

#### *3.3.5.1 Filtration Using Co-polyamide/FL-MXene Membrane*

Polyamide/FL-MXene placed in between the funnel and neck and the flask connected to a suction pump. Then turned on the pump and the oil samples filtered on by

one. First 10 ppm oil was filtered, while filtrate was collected in small glass bottle for spectroscopy measurement. The same procedure done for 100 ppm and 1000 ppm.

*3.3.5.2 Filtration Using Co-polyamide/ML-MXene Membrane*

The same steps followed for polyamide/ML-MXene membrane. Thus, the polyamide/ML-MXene placed in between the funnel and neck and sample filtered. The collected sample kept on small glass bottles for spectroscopy. The filtrate was colorless.

*3.3.5.3 Filtration Using Co-Polyamide Membrane*

Polyamide membrane used for filtration process. Followed the similar protocol, while polyamide membrane adjusted on glass filtration system and the sample filtered and collected for spectroscopy.

*3.3.5.4 Preparation of Standard Solutions of Oil for Plotting Calibration Curve*

The concentrations 50, 100, 250, 500 and 1000 ppm of vegetable oil in water were prepared. The transmission spectra were obtained using Libra biochrom spectrophotometer. The value of transmission for each concentration corresponding to 450 nm were measured. Transmission-Concentration chart plotted (Figure 26)

*3.3.5.5 Efficiency Calculations*

The values correspond to 450 nm for each concentration (10, 100, 1000 ppm) were obtained from the related spectra charts before and after filtration. Efficiency of samples measured using the following equation:

$$\text{eff.\%} = 100 - [\text{C (filtrate)}/\text{C (Stock solution)}] \times 100\%$$

Where eff% is representing the separation efficiency in %, c(filtrate) indicates the oil concentration in the filtrate in ppm and c(stock solution) is the oil concentration in stock solution.

### 3.4 Scanning Electron Microscopy (SEM)

The surface morphology of the specimens was examined with a field emission scanning electron microscope (FEI-SEM, Nova Nano SEM 450) equipped with energy-dispersive X-ray spectroscopy (EDS) with secondary electron images at 3 kV and different magnifications. All specimens were sputter-coated with 2 nm of gold before SEM images were taken.

### 3.5 Transmission Electron Microscopy (TEM)

To get higher resolution image of few-layer MXene HR-TEM FEI. TECNAI G TF 20 was used. The specimens were dispersed well in deionized water using sonication bath for 20 minutes.

### 3.6 Contact Angle Measurement

The OCA35 optical system (Data Physics, Germany) was used to measure the wettability of prepared samples by the sessile drop technique. Liquids with a different surface tension (water, vegetable and diesel oil) were used to investigate wettability of the prepared PA samples. A volume of 1µL of each testing liquid was used to eliminate gravitational effects when studying the contact angle. A representative value of the contact angle was obtained from ten separate readings. The angle between the solid/liquid and liquid/vapor interface is referred to as the contact angle.

### 3.7 Profilometry Measurements

Leica DCM 8 profilometer was used to create three-dimensional optical surface morphology of synthesized fiber samples. Additionally, Sa (arithmetical mean height) that represents information on the surface roughness was recorded. Up to 70° shapes and steep inclinations examining of complex done by utilizing non-destructive confocal technology

on surface of sample. The confocal images results from a very sensitive detector with high resolution up to 1.4 million pixels. Inclusive data from the sample surface with high disparity can be scanned.

### 3.8 Atomic Force Microscopy

Atomic Force Microscopy (AFM) was used to further elucidate 2D and 3D surface morphology of electrospun nanofibers using MFP3D Asylum research (USA) equipped with a Silicon probe (Al reflex coated Veeco model – OLTESPA, Olympus; spring constant: 2 N m–1, resonant frequency: 70 kHz). Measurements were performed under ambient conditions using the Standard Topography AC air (tapping mode in air). An AFM head scanner applied with Si cantilever adjacent vertically in the sample resonant frequency of the free-oscillating cantilever set as the driving frequency.

### 3.9 UV Spectroscopy

Libra biochrom spectrophotometer was used for transmittance measurements. The transmittances spectra for various oil concentration and filtrates were created by the machine for wavelength range between 200 nm and 800 nm, then the values corresponding to 450 nm were obtained.

# CHAPTER 4: RESULTS & DISCUSSION

This section divided into two parts, first discuss the results related to the sensors and second results of membrane.

The process of sensor fabrication displayed in Figure 2. The gold electrode was covered with ES mat of 13 wt.% SIS and 10 wt.% CNTs using electrospinning method to get SIS/CNT sensor followed by drying in the oven for 24 hours under 60 °C.

Figure 3 demonstrates the fabrication of coPA/MXene membrane starting from preparation of coPA membrane by electrospinning of coPA solution in n-propanol then in the next step adding MXene particles to coPA membrane using glass filtration system technique to obtain coPA/ML and FL-MXene membranes.

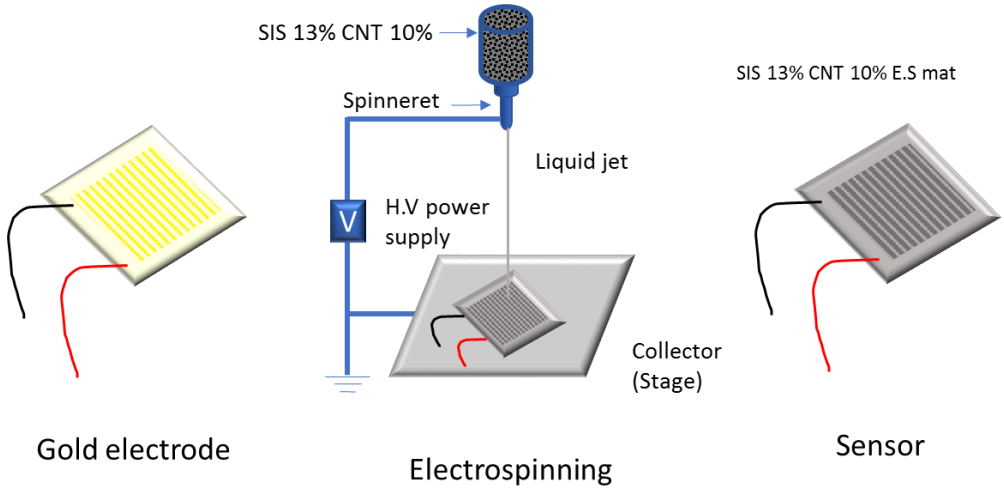


Figure 2 Illustration of fabrication of sensor by electrospinning of 13 wt.% of SIS and10 wt.% of CNT on gold electrode.

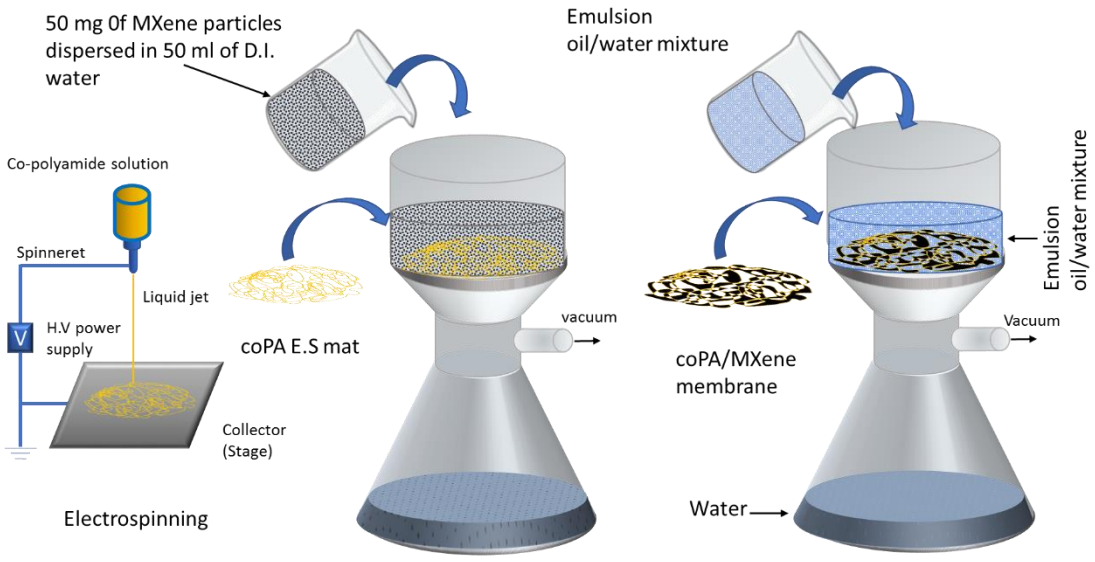


Figure 3 Schematic of fabrication of coPA/MXene electrospun mat and emulsion oil/water separation process

## 4.1 Sensors Characterization and Resistivity Measurements

### *4.1.1 SEM Characterization of SIS Membranes*

As a first approach, SIS polymer was dissolved in toluene. Different concentrations of SIS were electrospun to find the optimum concentration and condition for producing fibers, but no fiber produced.

In the next step, SIS-CNTs solutions were prepared to see the ability of creating fibers when SIS is mixed with CNTs. However, no fiber appeared in all conditions.

As a second approach, the mixture of tetrahydrofuran and dimethylformamide was selected, since THF/DMF was previously used in published works to obtain electrospun fibers of SIS. Various concentrations of SIS (from 10 to 15% were prepared in THF:DMF 50:50 (v/v) and THF:DMF 80:20 (v/v). Good fibers were created for SIS in THF:DMF 80:20 (v/v) while the solutions of SIS in THF:DMF 50:50 (v/v) were too viscous and not

satisfied for doing electrospinning. The best fiber quality was obtained from 13 and 15 wt.% of SIS as it shown in Figure 4 and Figure 5. As it clear in Figure 5(a) and (b) the fiber produced clearly on the size of hundreds nanometer.

In the next step, various concentration of CNTs (0.5, 1, 2.5, 5 and 10 wt.% of CNTs) were dispersed in the SIS solutions and electrospinning was performed.

Figure 6 (a and b) represents the SEM result of 13 wt.% of SIS and 1 wt.% of CNT after electrospinning under 10 and 15 KV with flow rate of 1 ml per 1 hr. The best electrospun mat was obtained from 13 wt.% of SIS and 10 wt.% of CNT much better than 15 wt.% of SIS and 10 wt.% of CNT which was containing some beads as shown in Figure 7. In addition, 13 wt.% of SIS and CNT 10 wt.% displayed perfect uniform fiber size with no defects and voids in the membrane structure.

a) 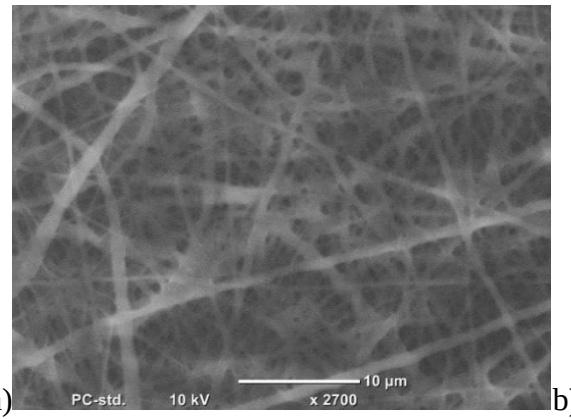

b) 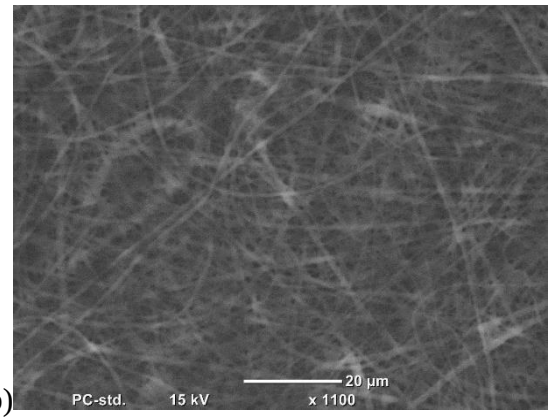


Figure 4 SEM image of 15 wt.% of SIS in THF/DMF 80:20 (v/v) 15KV a) 20KV b) 25KV

a) 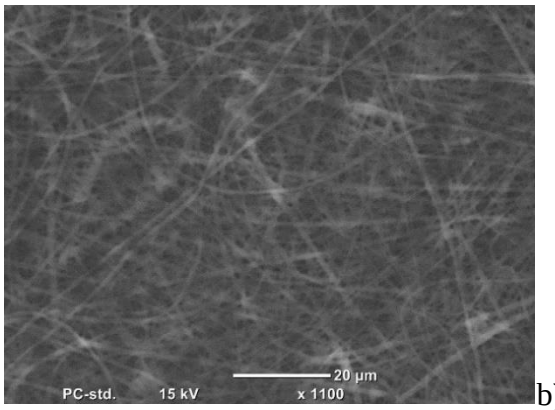

b) 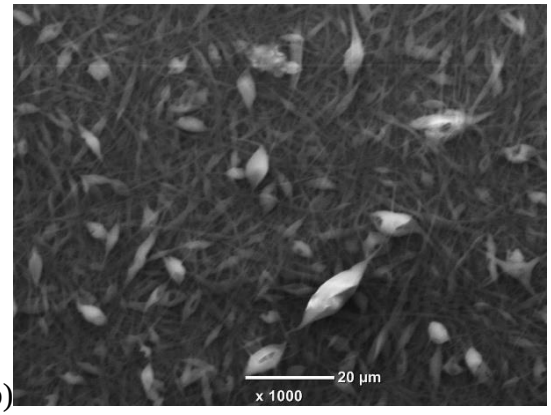


Figure 5 SEM image of 13 wt.% OF SIS in THF/DMF 80:20 (v/v) electrospun by loading 15 KV a) 13 wt.% SIS b) 15 wt.% SIS

a) 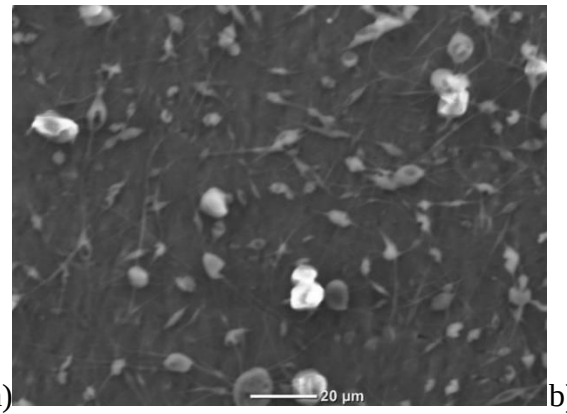

b) 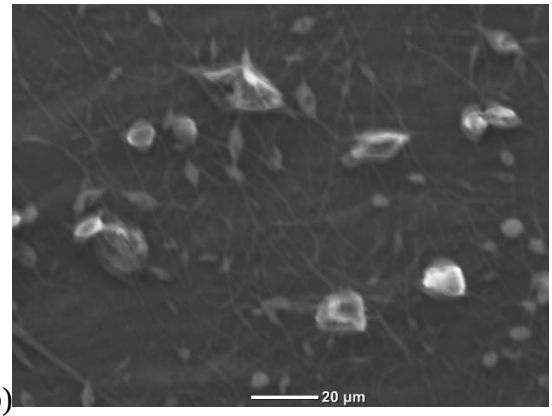


Figure 6 SEM image of 13 wt.% of SIS in THF/DMF 80:20 (v/v) 1 wt.% CNT a) 10 KV b) 15 KV

a) 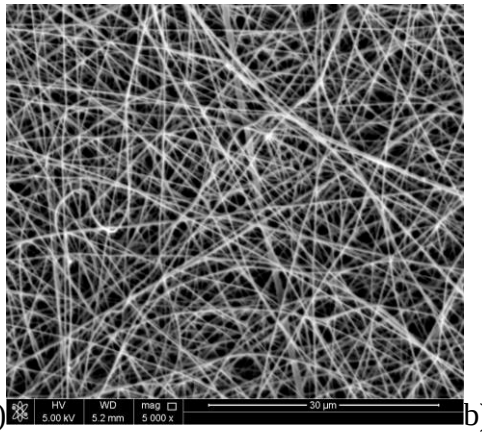

b) 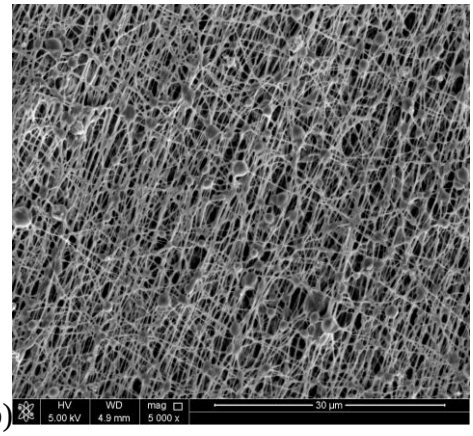


Figure 7 SEM image of a) 13 wt.% of SIS and 10 wt.% of CNT b) 15 wt.% of SIS and 10 wt.% of CNT

### *4.1.2 Oil Absorption Capacity of Casted Film and Electrospun Mat of SIS*

Oil absorption capacity were tested on casted and electrospun SIS polymer. In case of electrospun SIS, 3.31g of oil per 1g of SIS was absorbed within first hour with no further absorption.

In case of casted film, absorption capacity increased about 10 time from 0.35 g of oil per 1g of film after 1 hour of immersing to 3.34 g of oil per 1g of film after 20 hours of immersing of the oil. Thus, the electrospun mat of SIS are expect to have an advantage for sensor application compare to film due to fast oil absorption.

Gold interdigitated electrodes were chosen for fabricating the sensors. The electrodes was covered by electrospun mat of 13 wt.% of SIS 2.5, 5 and 10 wt.% of CNT for 30 min until they completely covered with the mat and similarly also coated with casted film of same concentrations (Figure 8). Average weight of the sensors used for sensing experiments was 10 mg ± 2 mg and average thickness of sensors was 100 µm ± 10 µm were measured.

a) 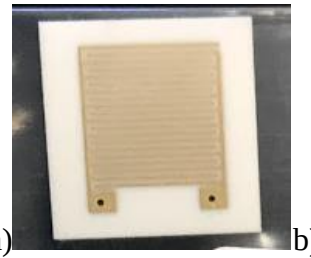 b) 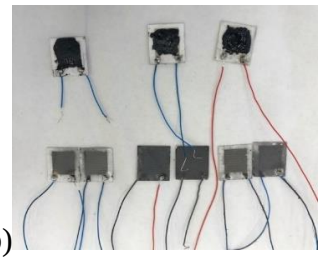 c) 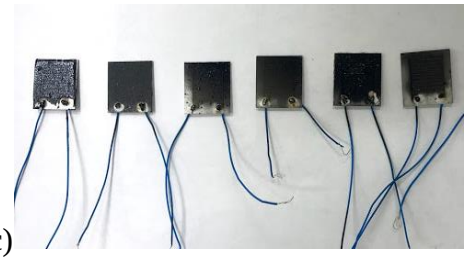

Figure 8 Gold interdigitated electrode (a), Gold electrodes coated with 13 wt.% of SIS fiber 2.5, 5 and 10 wt.% of CNTs using electrospinning technique (b & c).

### *4.1.3 Resistivity Measurements*

The 13 wt.% of SIS CNTs were electrospun on gold interdigitated electrodes. The 13 wt.% of SIS and 10 wt.% of CNT sensors exposed to toluene and acetone vapors. The resistivity was measured by time as Figure 9a. shows the relative resistivity increasing until reaching the plateau point, which means that the vapors absorbed by the SIS mat swelled resulting in segregation of carbon nanotubes what leads to increase of resistivity. Toluene get earlier to equilibrium than acetone, it took five minutes while acetone after six minutes, which shows that absorption of toluene is faster than acetone.

Figure 9 b. represents the relative resistivity changes by time for water and oil. Water did not effect resistivity whereas the sensor resistivity increases dramatically after adding oil and after 3 minutes was reached to plateau.

Figure 9c represents the resistivity changes of 13 wt.% of SIS and 10 wt.% of CNT for several concentrations of vegetable oil. The resistivity of SIS-CNTs sensor increase by increasing the concentration. The higher oil concentration caused the plateau faster than lower concentrations. Hence, faster sensor response due to higher oil concentration. This happens due to swelling of SIS mat resulted from absorbing of oil which further causing in the CNTs disconnected.

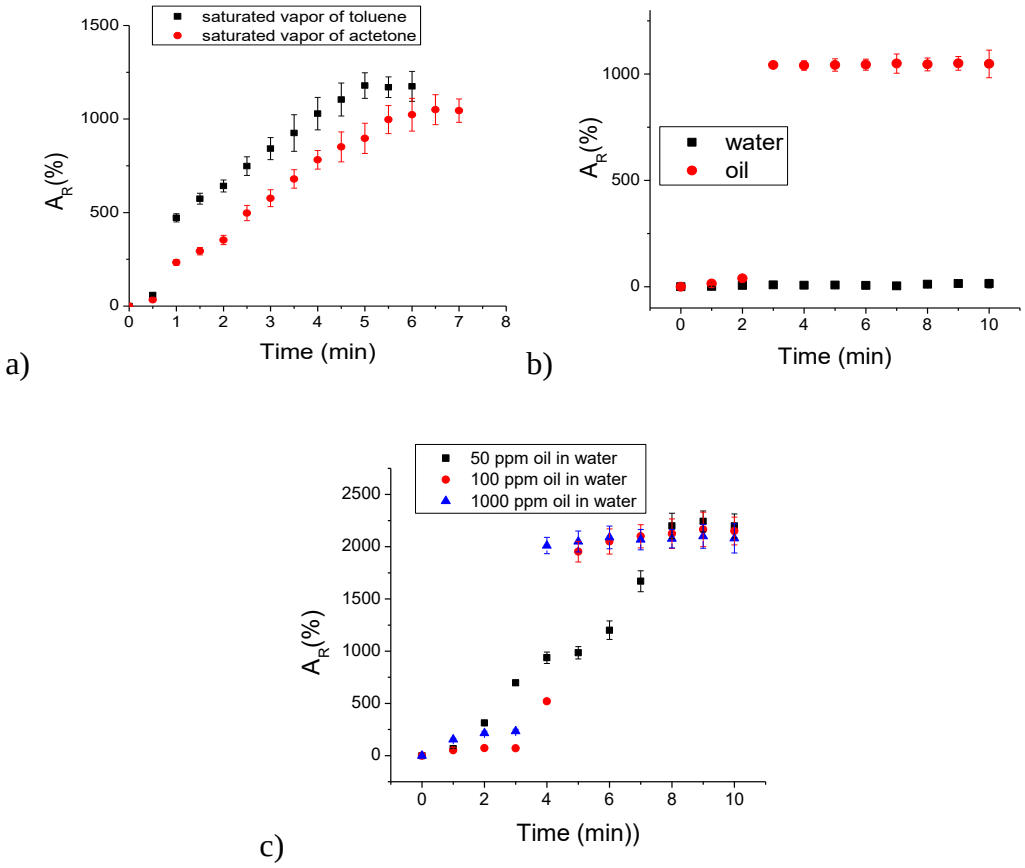


Figure 9 Resistivity changes of 13 wt.% of SIS and10 wt.% of CNTs a) toluene and acetone, b) water and pure vegetable oil and c) 50,100 and 1000 ppm vegetable oil

## 4.2 Result and Discussion of Membrane Part

### *4.2.1 MXene Acid Etching*

Etching process of MAX phase is shown in Figure 10. Aluminum layer was remove via etching of MAX phase using strong HF acid created in situ (LiF+HCl) resulting in $Ti_3C_2T_x$.

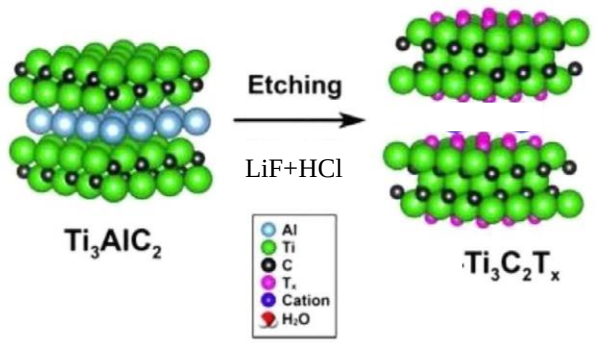


Figure 10. Schematic illustration of etching of MAX phase [135].

### *4.2.2 MXene Delamination*

Delamination of MXene multilayer structure was done by ultrasonic bath, the layers are separated to give FL-MXene (Figure 11 b).

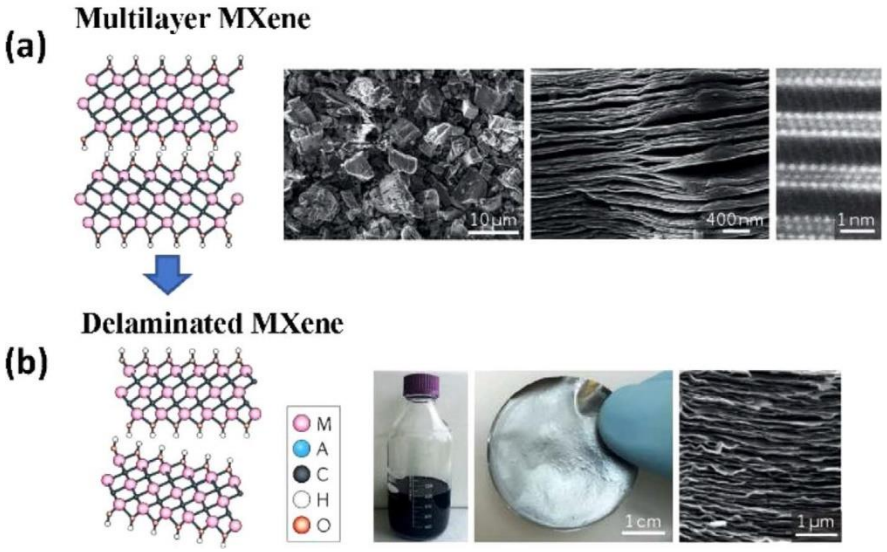


Figure 11 (a) Illustrations of multilayered MXene. From left to right, (b) Illustrations of delaminated MXene. From left to right [18]

### *4.2.3 Characterization and Separation Efficiency of MXene and CoPA-MXene membranes*

#### *4.2.3.1 Scanning Electron Microscopy*

Figure 12 represents the SEM image of MAX phase ($Ti_3AlC_2$). It is clearly visible that MAX phase contains multiple layers structure stack together.

Strong etching using mixture of LiF and HCl removes the Al layers from the MAX phase, gaps appear between the layers but still joining together due to the residual forces which keep layer connected resulted in multilayer-MXene ($Ti_3C_2T_X$) (Figure 13).

Delamination of ML-MXene by sonication consequences in braking the weak residual forces therefore separation of ML-MXene and formation of single layer-MXene (Figure 14) in shape of small particles (lateral size around few 100 nanometers).

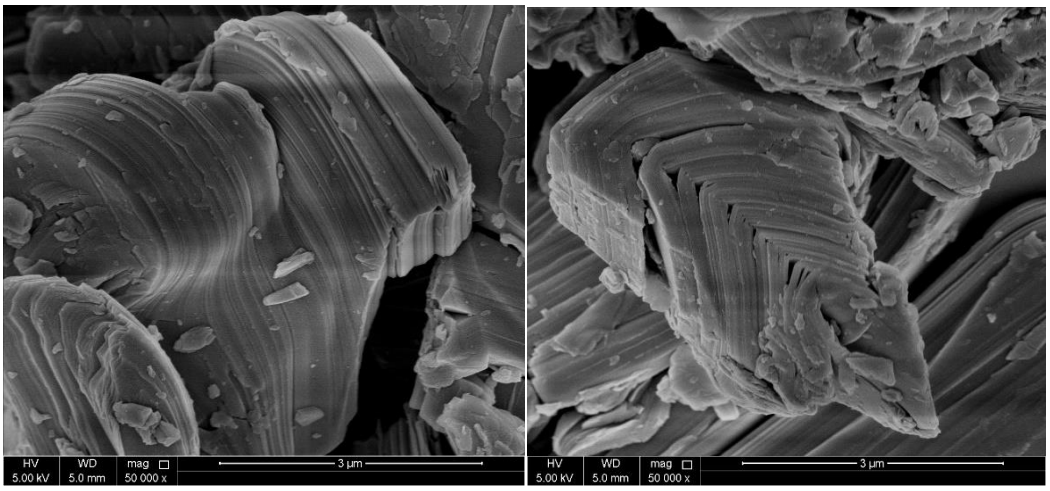


Figure 12 SEM image for MAX phase from natural stone

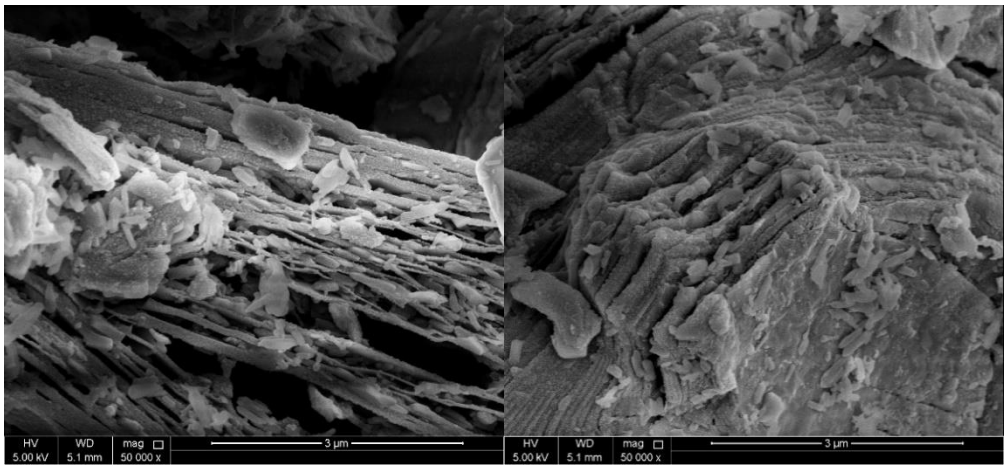


Figure 13 SEM image of ML-MXene produced after acid etching

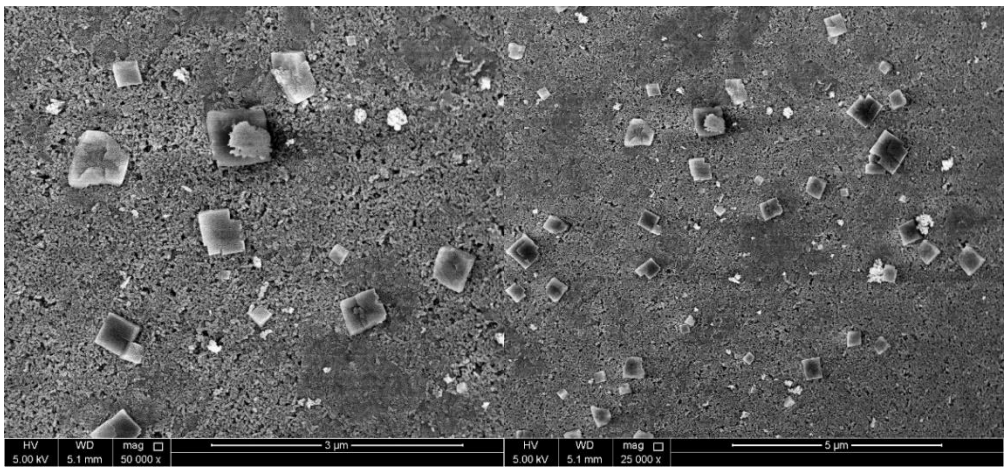


Figure 14 SEM image of few layer MXene with different magnification after delamination

*4.2.3.2 Transmission Electron Microscopy (TEM)*

High resolution -TEM was employed to study structure of prepared MXene particles. TEM images represented the small particles in size of few nanometer. After delamination using sonication bath the ML-MXene layers separated to few or single layers. (Figure 15)

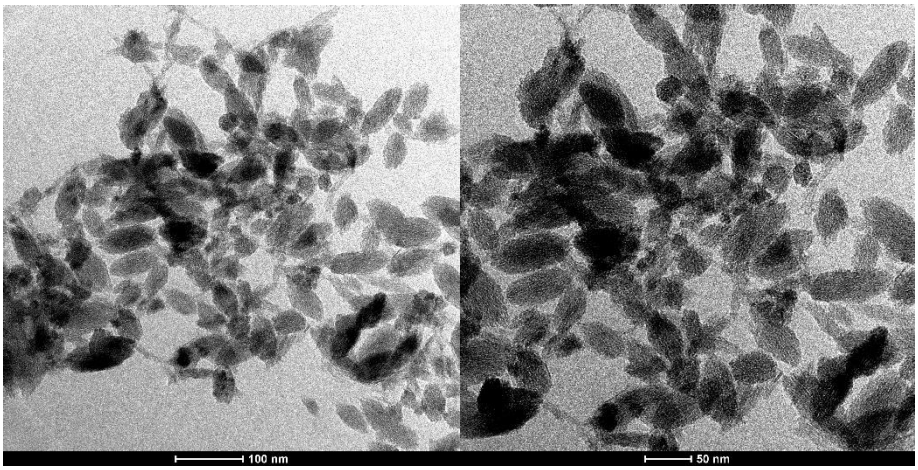


Figure 15 TEM image of FL-MXene

*4.2.3.3 Energy Dispersive x-ray Spectroscopy (EDX)*

To obtain the composition of elements in MAX phase, ML-MXene and FL-MXene elemental analysis or chemical characterization was done by utilizing EDX analytical technique. Figure 16 representing the EDX image of MAX phase ($Ti_3AlC_2$). The graph is plotted base on counts per second and energy (eV). There are peaks correspond to 0.25 and 4.5 eV which is indicate existence of Ti and a peak next to 1.5 eV represents presence of Al elements, carbon peak appeared close to 0.1 eV. The Al wt.% is 6.93 of total and the at.% is 9.69 (Table 3).

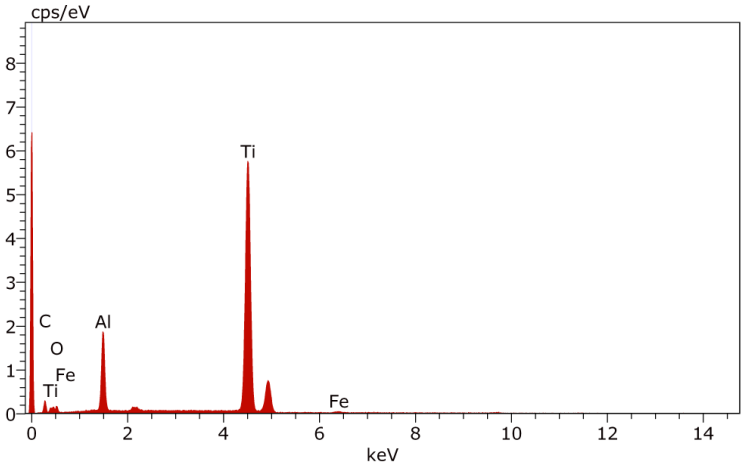


Figure 16 Illustration of EDX graph for MAX phase

Table 3. *EDX results for MAX phase*

| Element | norm. C [wt.%] | Atom. C [at. %] |
|---|---|---|
| C | 3.79 | 11.93 |
| O | 5.16 | 12.17 |
| Al | 6.93 | 9.69 |
| Ti | 83.17 | 65.57 |
| Fe | 0.95 | 0.64 |

Figure 17 illustrating the EDX image for ML-MXene, the Al layer removed by strong etching with HF and HCl. The same peaks appeared as the MAX phase EDX image shown extra to these some new peaks also appeared on EDX image after etching correspond to 0.7 and 2.6 eV which are for Cl and F respectively that introduced to the MXene structure from the acid and staid at MXene terminals. The wt.% and at. % of aluminum decreased to 1.7 and 1.96 of total respectively while 22.11 wt.% of F atoms added to the MXene structure (Table 4).

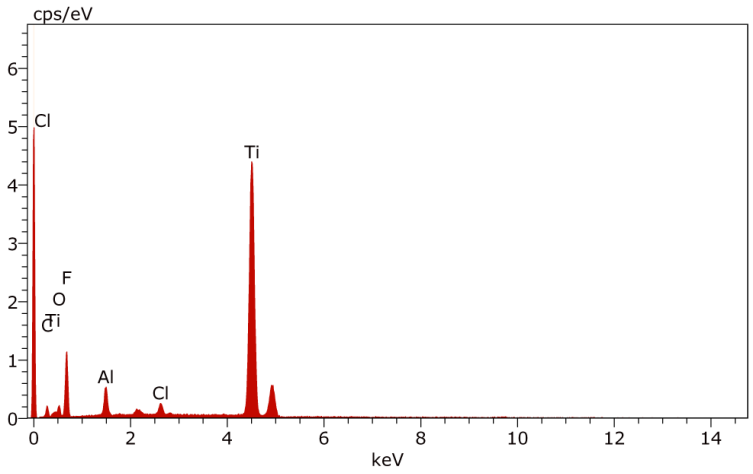


Figure 17 EDX graph for ML- MXene

Table 4. *EDX result for ML-MXene after acid etching of MAX phase*

| Element | norm. C [wt.%] | Atom. C [at. %] |
|---|---|---|
| C | 2.57 | 6.59 |
| O | 6.13 | 11.83 |
| F | 22.11 | 35.92 |
| Al | 1.71 | 1.96 |
| Cl | 0.81 | 0.70 |
| Ti | 66.67 | 42.99 |

During delamination process the residual forces between the layers broke to from FL- MXene the EDX image shows peaks at 0.25 and 4.5 eV for Ti, 0.7 and 0.1 eV for F and C respectively with no peak for Al which proofs sucesful delamination (Figure 18). Al element disappeared completely after sonication that represents produce of FL-MXene due to delamination. (Table 5)

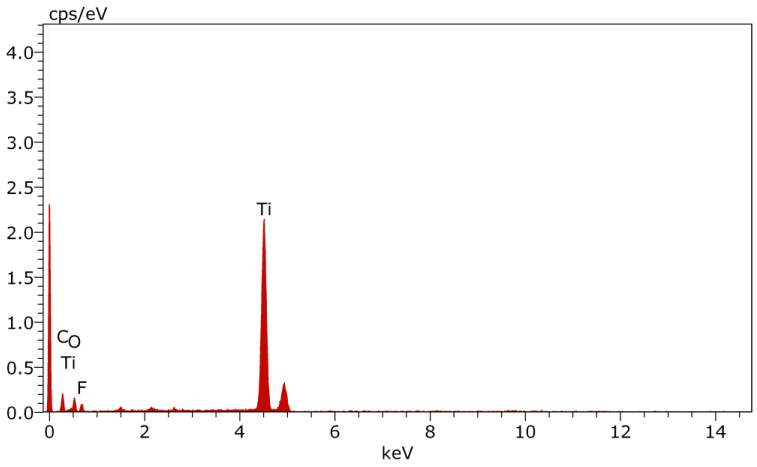


Figure 18 EDX graph for FL-MXene after delamination of ML-MXene

Table 5. *EDX result for FL-MXene produced after delamination of ML-MXene*

| Element | norm. C [wt.%] | Atom. C [at. %] |
|---|---|---|
| C | 5.95 | 15.87 |
| O | 12.67 | 25.35 |
| F | 4.30 | 7.25 |
| Ti | 77.08 | 51.53 |

The prepared membranes are displayed in Figure 19. Co-polyamide mat coated with ML-MXene and FL-MXene. MXene particles distributed homogenously inside and on coPA membrane.

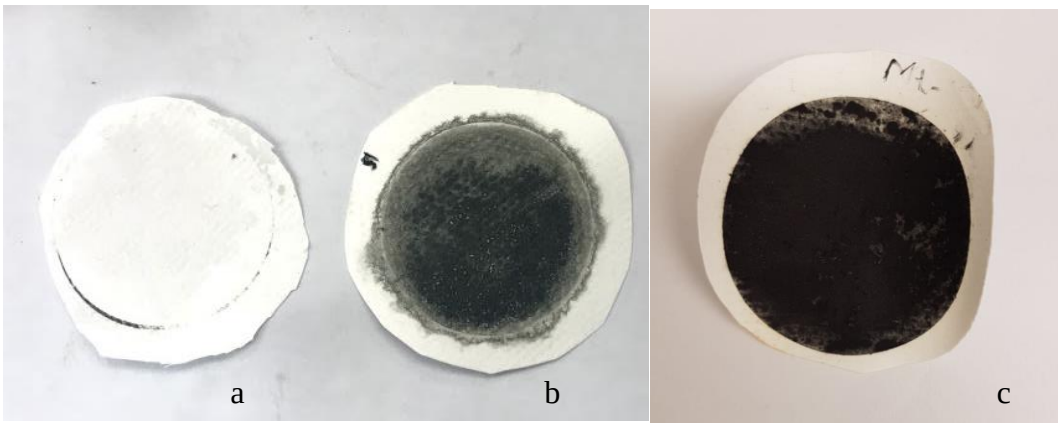


Figure 19 Polyamide membrane (a), Polyamide/single layer-MXene membrane (b) and Polyamide/multi-layer-MXene membrane (c)

#### *4.2.3.4 Atomic Force Microscopy*

Topography of membranes surfaces was study by AFM technique. Figure 20(a) shows the AFM image for coPA. As it is obvious the fiber strains wove in very clear shape and created many pores in various size. The pores are not filled, what makes the oil molecules pass through membrane. Figure 20(b) represents the topography of coPA/ML-MXene membrane. The fiber is coated with ML-MXene, the surface of membrane is covered by the MXene particles and the pores are becoming quite tight for neat vegetable oil molecules to pass through it. Figure 20(c) indicates the topography of coPA/FL-MXene membrane in which coPA membrane coated by FL-MXene. The particles settled inside the pores and on the fiber. In this membrane, the vegetable oil facing FL-MXene obstacle to permeate through the membrane and most of it will absorb with the FL-MXene. Thus, The FL-MXene less permeable to oil molecules, what made efficiency of separation high for coPA/FL-MXene as same as coPA/ML-MXene.

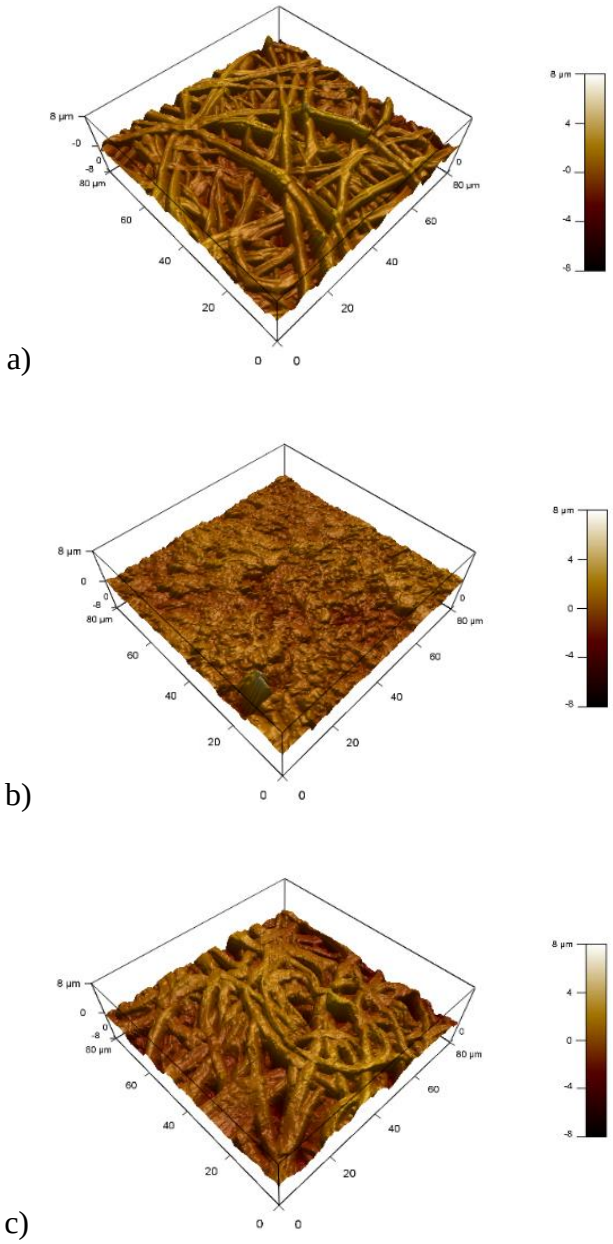


Figure 20 AFM images of a) neat coPA membrane, b) coPA membrane coated by ML MXene and c) coPA membrane coated by FL MXene

### *4.2.3.5 Profilometry Measurement*

Polyamide fiber showed regular and homogeneous structure with no appearance of beads. The value of Sa for pure polyamide fibers was 0.87 μm whereas the Sa value for

FL-MXene and ML-MXene were 1.82 µm and 1.46 µm respectively which represents that adding FL-MXene and ML-MXene to coPA fiber result in sharp increase in surface roughness (Figure 21).

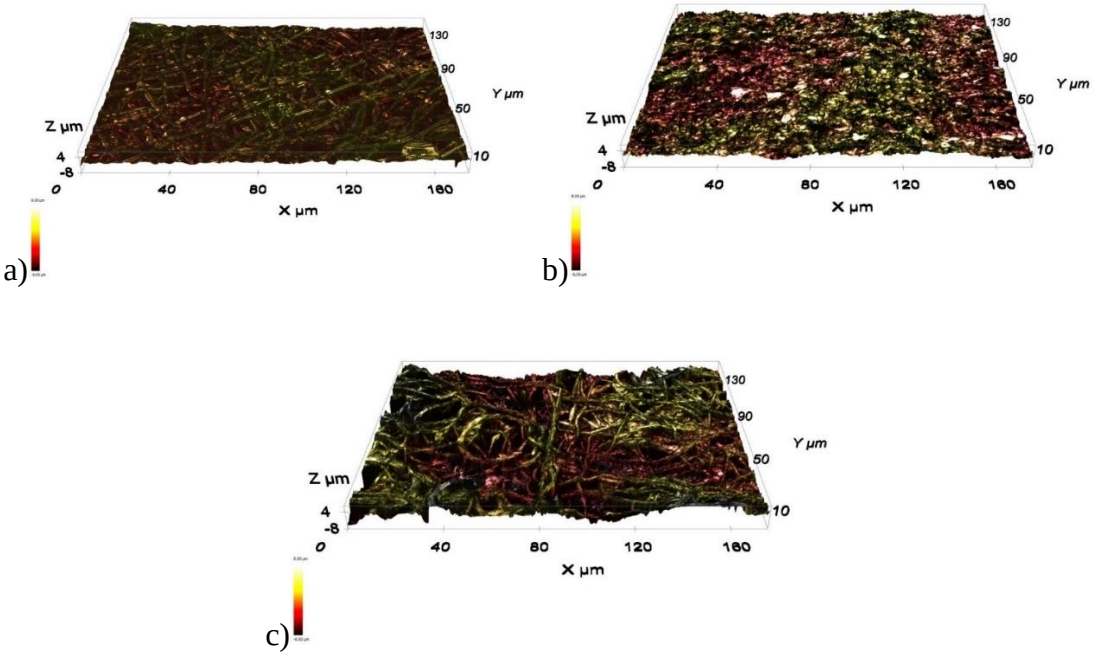


Figure 21 Profile measurement of a) neat coPA membrane, b) coPA membrane coated by ML MXene and c) coPA membrane coated by ML MXene

Figure 22a displays profilometry measurement of coPA and coPA/ML-MXene. The average thickness of coated ML-MXene on membrane was about 35µm. Whereas, the average thickness of coated FL-MXene on membrane was 30 µm (Figure 22)

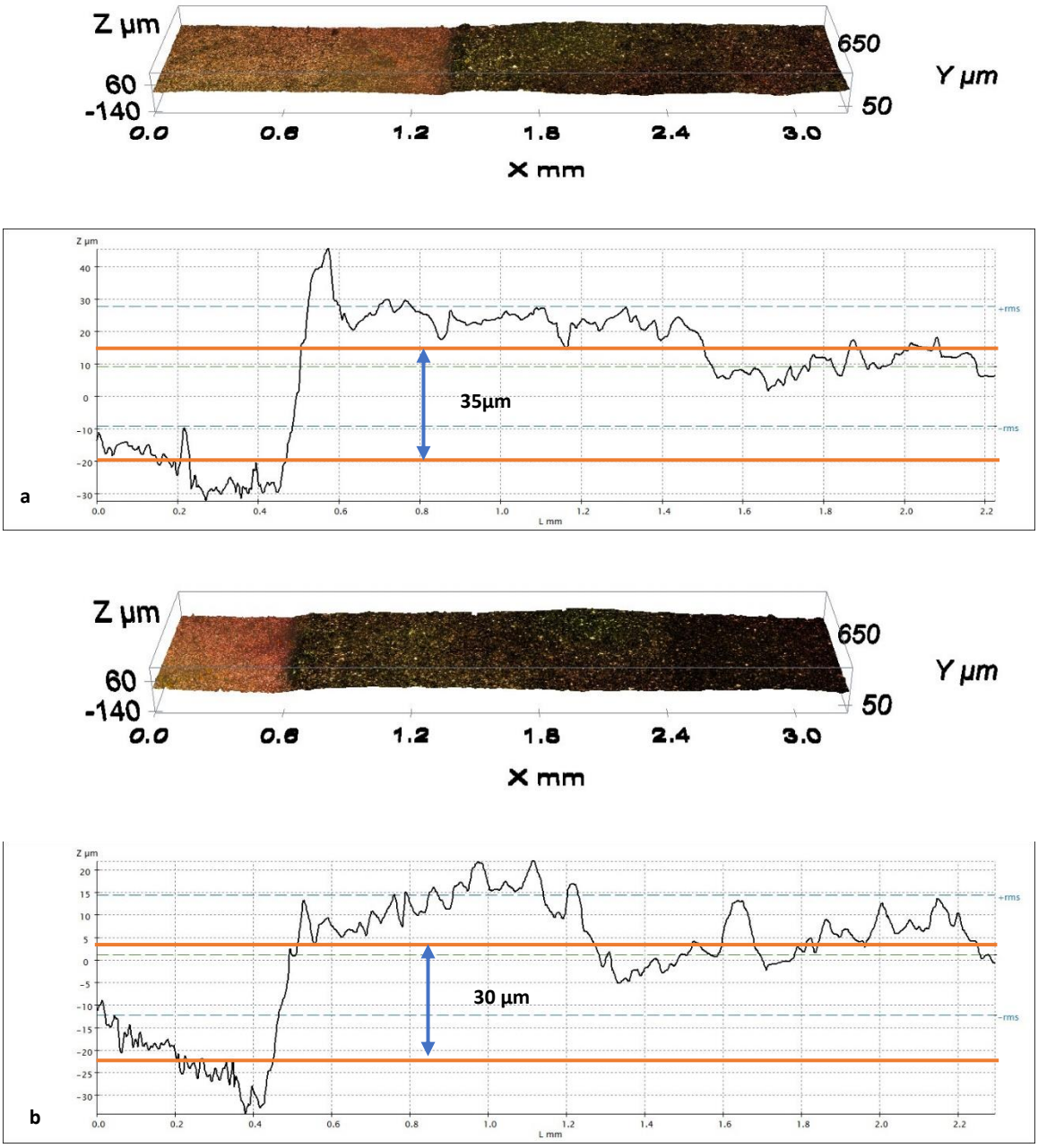


Figure 22 a) Profilometry of coPA and coPA/ML-MXen with line graph b) coPA and coPA/FL-MXene with its line graph

*4.2.3.6 Contact Angle Measurements*

Wettability strongly depends on chemical nature (polar or nonpolar) and surface roughness. In Figure 23, the contact angle of water, formamide, ethylene glycol and oil with the coPA, coPA/ML-MXene and coPA/FL-MXene are shown. Co-polyamide due to including -CO and -NH functional groups on its structure is considered to be hydrophilic polymer. The contact angle of water, formamide, ethylene glycol and oil on pure coPA membrane was 42, 4, 1 and 8° respectively. Contact angle of water, formamide, ethylene glycol and oil on coPA/ML-MXene membrane was 100, 20, 45 and 3° respectively and 130, 111, 15 and 5° are the contact angle values for water, formamide, ethylene glycol and oil coPA/FL-MXene. From theoretical point of view, the contact angle of polar solvent must be less on hydrophilic surfaces. In our case, we suppose that the high surface roughness strongly influencing contact angle.

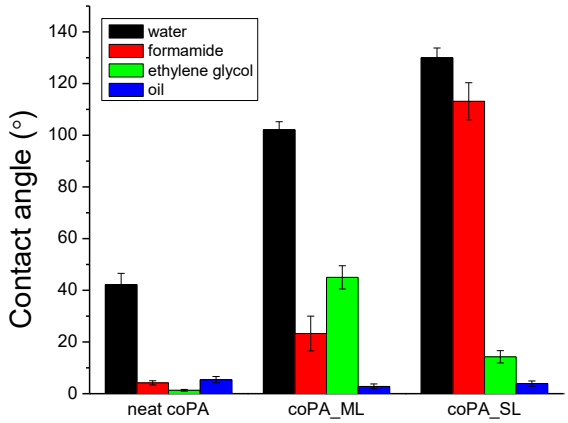


Figure 23 Contact angle for different solvents on coPA, co-polyamide-Multi Layered-MXene and coPA few-layered MXene

Casted films of ML and FL Mxene were prepared in order to eliminate roughness parameter. Moreover, the measurement of contact angle of oil was done under water to mimicking real condition during oil water separation. The average contact angles of vegetable oil on FL-MXene and ML-MXene casted films were 159.95° and 132.52° respectively, which are quite high, prove oleophobicity of MXene layers. This property of MXene is essential in oil removal from water (Figure 24).

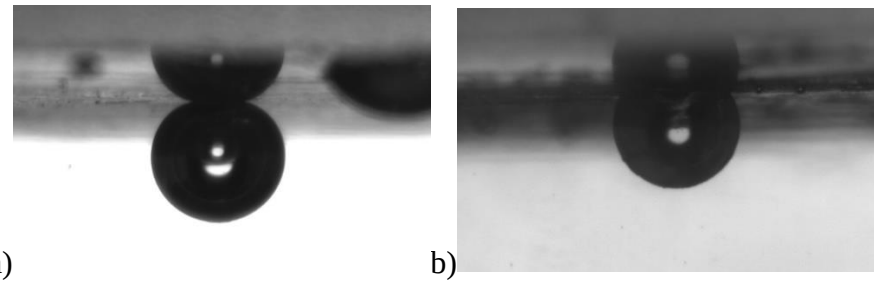

a) b)

Figure 24 Contact angle of vegetable oil on a) FL-MXene and b) ML-MXene casted films under water.

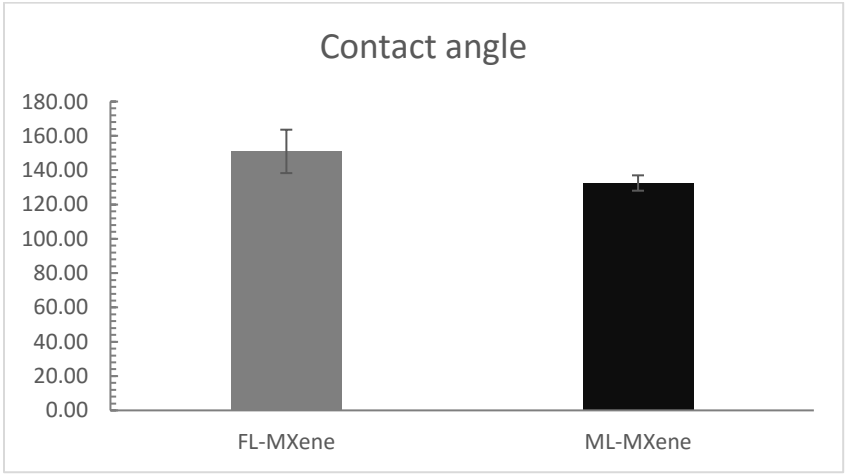


Figure 25 Contact angle results for VO on casted film of FL-MXene and ML-MXene

The results indicate that the average value of contact angle of vegetable oil on FL-MXene underwater is higher than its relative for ML-MXene. It means that FL-MXene is more oleophobic towards vegetable oil comparing to ML-MXene (Figure 25).

### *4.2.4 Spectroscopy Results*

#### *4.2.4.1 Calibration Curve*

In order to estimate concentration of oil in filtrates calibration fits were done by preparing of mixtures of oil in water with various concentration Figure 26. The values of transmittance of standard mixtures correspond to 450 nm were collected, plotted and subsequently values was linear fitted [42]. Subsequently, Beer-Lambert law was used to calculate particular concentration of oil in filtrate.

According to the Beer-Lambert law the amount of light absorbed by a substance dissolved in a totally transmitting solvent directly proportional related to the path of solution and the concentration of substance.

$$\mathbf{A = \varepsilon\, l\, c}$$

Where, A is absorbance, ε is wavelength dependence absorptivity coefficient (molar absorptivity), l is representing path length and c is indicating the solution concentration.

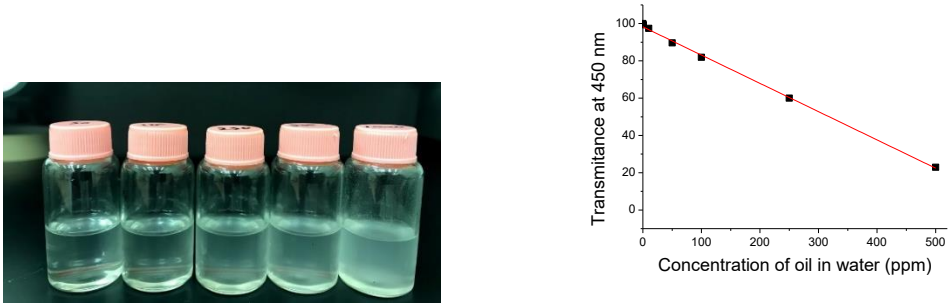


Figure 26 Calibration curve T% versus concentration (ppm)

### *4.2.5 Water/oil Separation Efficiency*

Figure 27a. shows different concentrations of oil before filtration and figure 27b. filtrates after separation.

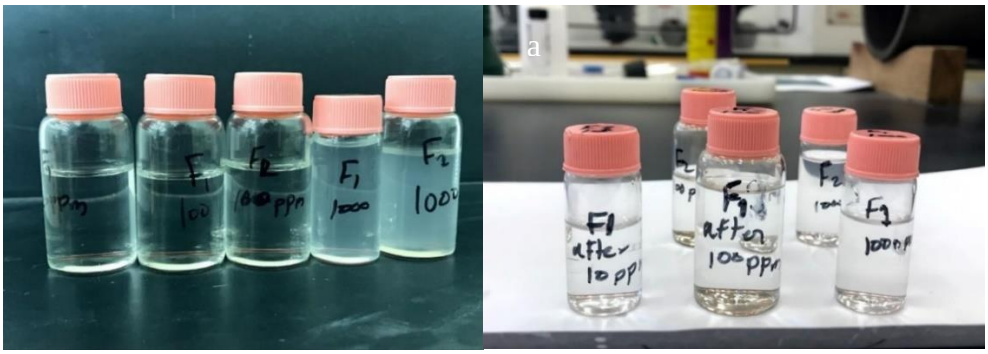

Figure 27 Different oil samples before filtration (a), Oil samples after filtration using polyamide/FL-MXene membrane

Figure 28 shows the separation efficiency plotted for different membranes toward different concentrations. The efficiency for 10 ppm vegetable through the co-polyamide membrane showed only 18% separation efficiency while coPA/ML-MXene exhibited efficiency around 99.5% and the separation efficiency increased up to 99% for coPA/FL-MXene. Thus, the coPA more permeable to 10 ppm neat vegetable oil and only 20% efficient while separation efficiency for coPA/ML-MXene and coPA/FL-MXene goes up to 99.5% for neat oil 10 ppm. Figure 28(a). Figure 28(b & c) shows the efficiency for 100 ppm and 1000 ppm neat oil separation. The coPA membrane represents separation efficiency up to 70 % and 99 % and 98 % for coPA/ML-MXene and coPA/FL-MXene. Similar values of efficiency for neat vegetable oil 1000 ppm. According to Sobolciak et al. the oil water separation depends on absorption of oil inside the membranes[42].

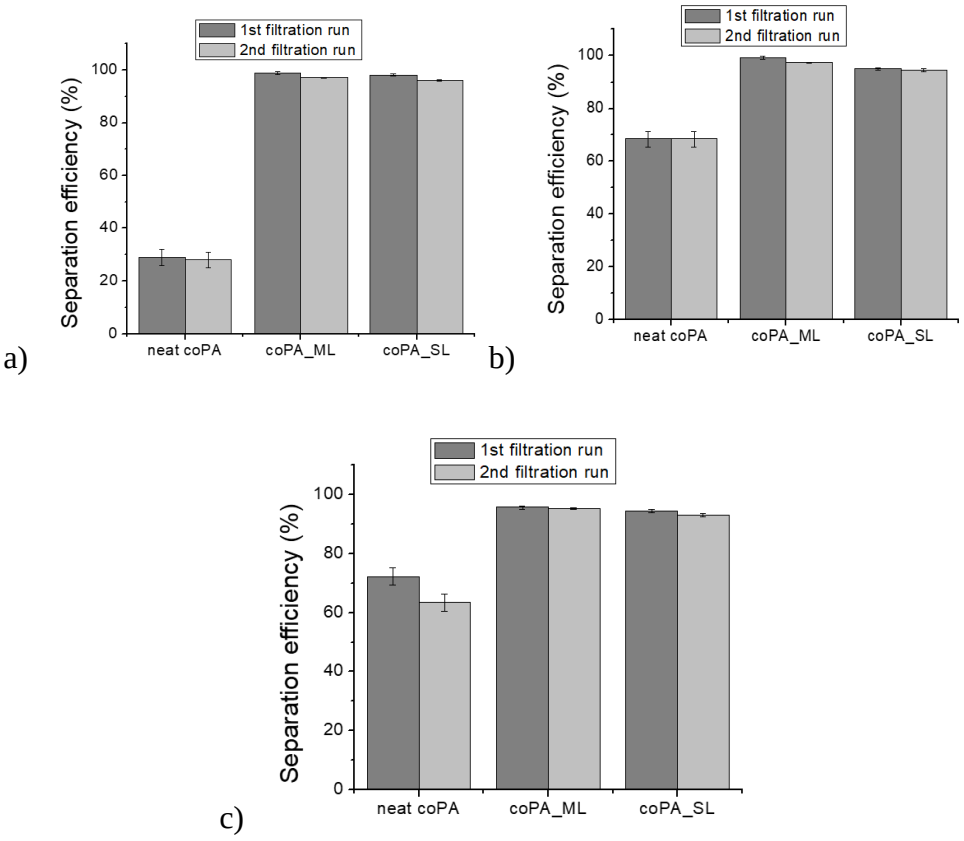


Figure 28 UV spectroscopy of filtrates obtained after separation of a) 10, b) 100 and c) 1000 ppm vegetable oil in water through neat coPA and coPA coated with MXene membranes

### *4.2.6 Flux of Dispersions Through Membranes*

Flux of dispersion through membrane decreasing with increasing the oil concentration. Figure 29a is showing flux of dispersion through coPA/ML-MXene at 0.5 bar. Flux for 10 ppm is around 10000 L/m$^2$h, decreases to 7000 L/m$^2$h for 100 ppm and about 3500 L/m$^2$h for 1000 ppm. The similar trend, decreasing of flux with increasing concentration of oil was observed for coPA/FL-MXene (Figure 29 b).

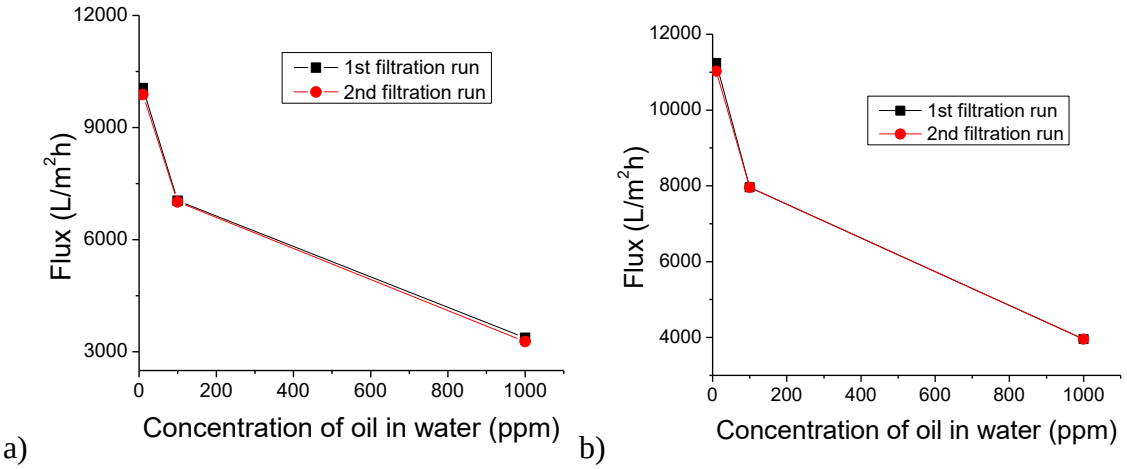


Figure 29 Flux of dispersions through membrane a) coPA ML-MXene b) coPA FL-MXene

# CHAPTER 5: CONCLUSIONS

## 5.1 Sensors

- Electrospinning technique was used to obtain mat from SIS and SIS/CNT composites deposited on the gold electrodes.
- The best mats in terms of fibers uniformity and resistivity values suitable for sensing experiments was obtained from 13 wt.% of SIS and 10 wt.% of CNT.
- The prepared sensors were responding to solvent vapors and oil content.
- Vapor sensing were done for toluene and acetone. Sensors exhibited fast response, where time to reach a plateau for toluene was 5 min, whereas 6 min for acetone vapors.
- Prepared sensors were successfully used for sensing of oil in water. The lowest concentration of oil in water possible to qualitatively determinate was 50 ppm.

## 5.2 Membranes

- MXene was prepared successfully through etching and delaminating of MAX phase. Prepared MXene particles were characterized by SEM, TEM and EDX.
- The measured contact angle of vegetable oil on MXene film under water showed the high oleophobicity of MXene particles, up to 152 º for FL MXene.
- Co-polyamide membrane prepared using electrospinning technique. Co-polyamide membranes were covered with MXene particles. Membranes were characterized by profilometry measurement, AFM, and contact angle measurement.
- coPA/MXene membranes showed high separation efficiency for oil in water separation, up to 98%, what indicates high potential of these type of membranes for separation oil from water. Prepared membrane exhibited high flux (up to 11000 $L/m^2h$) at 0.5 bar pressure of dispersion of water.

# REFERENCES

[1] V. N. Mochalin, O. Shenderova, D. Ho, and Y. Gogotsi, “The properties and applications of nanodiamonds,” *Nat. Nanotechnol.*, vol. 7, no. 1, pp. 11–23, Jan. 2012.

[2] N. Behabtu, C. C. Young, D. E. Tsentalovich, O. Kleinerman, X. Wang, A. W. K. Ma, E. A. Bengio, R. F. ter Waarbeek, J. J. de Jong, R. E. Hoogerwerf, S. B. Fairchild, J. B. Ferguson, B. Maruyama, J. Kono, Y. Talmon, Y. Cohen, M. J. Otto, and M. Pasquali, “Strong, light, multifunctional fibers of carbon nanotubes with ultrahigh conductivity.,” *Science*, vol. 339, no. 6116, pp. 182–6, Jan. 2013.

[3] D. S. L. Abergel, V. Apalkov, J. Berashevich, K. Ziegler, and T. Chakraborty, “Properties of graphene: a theoretical perspective,” *Adv. Phys.*, vol. 59, no. 4, pp. 261–482, Jul. 2010.

[4] S. Aryal, C. K. Kim, K.-W. Kim, M. S. Khil, and H. Y. Kim, “Multi-walled carbon nanotubes/TiO2 composite nanofiber by electrospinning,” *Mater. Sci. Eng. C*, vol. 28, no. 1, pp. 75–79, Jan. 2008.

[5] J. K. Y. Lee, N. Chen, S. Peng, L. Li, L. Tian, N. Thakor, and S. Ramakrishna, “Polymer-based composites by electrospinning: Preparation & functionalization with nanocarbons,” *Prog. Polym. Sci.*, vol. 86, pp. 40–84, Nov. 2018.

[6] F. Ejaz Ahmed, B. S. Lalia, N. Hilal, and R. Hashaikeh, “Underwater superoleophobic cellulose/electrospun PVDF–HFP membranes for efficient oil/water separation,” *Desalination*, vol. 344, pp. 48–54, Jul. 2014.

[7] M. Zoubeik, M. Ismail, A. Salama, A. H.-A. J. for S. and, and undefined 2017, “New developments in membrane technologies used in the treatment of produced water: A review,” *Springer*.

[8] H. Peng and A. Y. Tremblay, “Membrane regeneration and filtration modeling in treating oily wastewaters,” *J. Memb. Sci.*, vol. 324, no. 1–2, pp. 59–66, Oct. 2008.

[9] A. Rahimpour and S. S. Madaeni, “Polyethersulfone (PES)/cellulose acetate phthalate (CAP) blend ultrafiltration membranes: Preparation, morphology, performance and antifouling properties,” *J. Memb. Sci.*, vol. 305, no. 1–2, pp. 299–312, Nov. 2007.

[10] W. Chen, Y. Su, L. Zheng, L. Wang, and Z. Jiang, “The improved oil/water separation performance of cellulose acetate-graft-polyacrylonitrile membranes,” *J. Memb. Sci.*, vol. 337, no. 1–2, pp. 98–105, Jul. 2009.

[11] L.-F. Fang, S. Jeon, Y. Kakihana, J. Kakehi, B.-K. Zhu, H. Matsuyama, and S. Zhao, “Improved antifouling properties of polyvinyl chloride blend membranes by novel phosphate based-zwitterionic polymer additive,” *J. Memb. Sci.*, vol. 528, pp. 326–335, Apr. 2017.

[12] X. S. Yi, S. L. Yu, W. X. Shi, N. Sun, L. M. Jin, S. Wang, B. Zhang, C. Ma, and L. P. Sun, “The influence of important factors on ultrafiltration of oil/water emulsion using PVDF membrane modified by nano-sized TiO2/Al2O3,” *Desalination*, vol. 281, pp. 179–184, Oct. 2011.

[13] C. Paladiya and A. Kiani, “Nano structured sensing surface: Significance in sensor fabrication,” *Sensors Actuators, B Chem.*, vol. 268, pp. 494–511, 2018.

[14] D. Patranabi, *Sensors and Tranducers*. 2003.

[15] B. Noroozi and B. I. Morshed, “PSC Optimization of 13.56-MHz Resistive Wireless Analog Passive Sensors,” *IEEE Trans. Microw. Theory Tech.*, vol. 65, no. 9, pp. 3548–3555, Sep. 2017.

[16] A. P. Brokaw, “A temperature sensor with single resistor set-point programming,”

*IEEE J. Solid-State Circuits*, vol. 31, no. 12, pp. 1908–1915, 1996.

[17] A. Ajovalasit, "The Measurement of Large Strains Using Electrical Resistance Strain Gages," *Exp. Tech.*, vol. 36, no. 3, pp. 77–82, May 2012.

[18] J. Fraden, *Handbook of modern sensors: physics, designs, and applications*. 2004.

[19] R. C. Jorgenson and S. S. Yee, "A fiber-optic chemical sensor based on surface plasmon resonance," *Sensors Actuators B Chem.*, vol. 12, no. 3, pp. 213–220, Apr. 1993.

[20] S. C. Aung, R. C. K. Ngim, and S. T. Lee, "Evaluation of the laser scanner as a surface measuring tool and its accuracy compared with direct facial anthropometric measurements," *Br. J. Plast. Surg.*, vol. 48, no. 8, pp. 551–558, Jan. 1995.

[21] W. Muangrat, V. Yordsri, R. Maolanon, S. Pratontep, S. Porntheeraphat, and W. Wongwiriyapan, "Hybrid gas sensor based on platinum nanoparticles/poly(methyl methacrylate)-coated single-walled carbon nanotubes for dichloromethane detection with a high response magnitude," *Diam. Relat. Mater.*, vol. 65, pp. 183–190, May 2016.

[22] Y. Li, H. Liu, K. Dai, G. Zheng, C. Liu, J. Chen, and C. Shen, "Tuning of vapor sensing behaviors of eco-friendly conductive polymer composites utilizing ramie fiber," *Sensors Actuators B Chem.*, vol. 221, pp. 1279–1289, Dec. 2015.

[23] K. Li, K. Dai, X. Xu, G. Zheng, C. Liu, J. Chen, and C. Shen, "Organic vapor sensing behaviors of carbon black/poly (lactic acid) conductive biopolymer composite," *Colloid Polym. Sci.*, vol. 291, no. 12, pp. 2871–2878, Dec. 2013.

[24] J. Lu, B. Kumar, M. Castro, and J.-F. Feller, "Vapour sensing with conductive polymer nanocomposites (CPC): Polycarbonate-carbon nanotubes transducers with hierarchical structure processed by spray layer by layer," *Sensors Actuators B Chem.*, vol. 140, no. 2, pp. 451–460, Jul. 2009.

[25] X. M. Dong, R. W. Fu, M. Q. Zhang, B. Zhang, and M. Z. Rong, “Electrical resistance response of carbon black filled amorphous polymer composite sensors to organic vapors at low vapor concentrations,” *Carbon N. Y.*, vol. 42, no. 12–13, pp. 2551–2559, Jan. 2004.

[26] S. Zhao, W. Zhai, N. Li, K. Dai, G. Zheng, C. Liu, J. Chen, and C. Shen, “Liquid sensing properties of carbon black/polypropylene composite with a segregated conductive network,” *Sensors Actuators A Phys.*, vol. 217, pp. 13–20, Sep. 2014.

[27] S. G. Chen, J. W. Hu, M. Q. Zhang, M. W. Li, and M. Z. Rong, “Gas sensitivity of carbon black/waterborne polyurethane composites,” *Carbon N. Y.*, vol. 42, no. 3, pp. 645–651, Jan. 2004.

[28] N. Wang, Z. Xu, Y. Qu, G. Zheng, K. Dai, C. Liu, and C. Shen, “Liquid-sensing behaviors of carbon black/polyamide 6/high-density polyethylene composite containing ultrafine conductive electrospun fibrous network,” *Colloid Polym. Sci.*, vol. 294, no. 8, pp. 1343–1350, Aug. 2016.

[29] J.-F. Gao, D.-X. Yan, H.-D. Huang, X.-B. Zeng, W.-Q. Zhang, and Z.-M. Li, “Tunable positive liquid coefficient of an anisotropically conductive carbon nanotube-polymer composite,” *J. Polym. Res.*, vol. 18, no. 6, pp. 2239–2243, Nov. 2011.

[30] K. Kobashi, T. Villmow, T. Andres, L. Häußler, and P. Pötschke, “Investigation of liquid sensing mechanism of poly(lactic acid)/multi-walled carbon nanotube composite films,” *Smart Mater. Struct.*, vol. 18, no. 3, p. 035008, Mar. 2009.

[31] X. M. Dong, R. W. FU, M. Q. ZHANG, Z. P. Qin, B. Zhang, and M. Z. Rong, “Effects of Processing on Electric Response of Carbon Black Filled Poly(methyl methacrylate) Composites against Organic Solvent Vapors,” *Polym. J.*, vol. 35, no. 12,

pp. 1003–1008, Dec. 2003.

[32] Y. Qiu, J. Wang, D. Wu, Z. Wang, M. Zhang, Y. Yao, and N. Wei, "Thermoplastic polyester elastomer nanocomposites filled with graphene: Mechanical and viscoelastic properties," *Compos. Sci. Technol.*, vol. 132, pp. 108–115, Aug. 2016.

[33] H. Pang, L. Xu, D.-X. Yan, and Z.-M. Li, "Conductive polymer composites with segregated structures," *Prog. Polym. Sci.*, vol. 39, no. 11, pp. 1908–1933, Nov. 2014.

[34] L. Yang, Z. Wang, Y. Ji, J. Wang, and G. Xue, "Highly Ordered 3D Graphene-Based Polymer Composite Materials Fabricated by 'Particle-Constructing' Method and Their Outstanding Conductivity," *Macromolecules*, vol. 47, no. 5, pp. 1749–1756, Mar. 2014.

[35] D. Wu, Q. Lv, S. Feng, J. Chen, Y. Chen, Y. Qiu, and X. Yao, "Polylactide composite foams containing carbon nanotubes and carbon black: Synergistic effect of filler on electrical conductivity," *Carbon N. Y.*, vol. 95, pp. 380–387, Dec. 2015.

[36] Z. Tu, J. Wang, C. Yu, H. Xiao, T. Jiang, Y. Yang, D. Shi, Y.-W. Mai, and R. K. Y. Li, "A facile approach for preparation of polystyrene/graphene nanocomposites with ultra-low percolation threshold through an electrostatic assembly process," *Compos. Sci. Technol.*, vol. 134, pp. 49–56, Oct. 2016.

[37] D.-X. Yan, H. Pang, B. Li, R. Vajtai, L. Xu, P.-G. Ren, J.-H. Wang, and Z.-M. Li, "Structured Reduced Graphene Oxide/Polymer Composites for Ultra-Efficient Electromagnetic Interference Shielding," *Adv. Funct. Mater.*, vol. 25, no. 4, pp. 559–566, Jan. 2015.

[38] A.-J. Garcia-Sanchez, F. Garcia-Sanchez, and J. Garcia-Haro, "Wireless sensor network deployment for integrating video-surveillance and data-monitoring in precision

agriculture over distributed crops," *Comput. Electron. Agric.*, vol. 75, no. 2, pp. 288–303, Feb. 2011.

[39] S. Mola, M. Magini, and C. Malvicino, "Equivalent Temperature Estimator Using Mean Radiant Temperature Sensor," *Meas. Control*, vol. 34, no. 6, pp. 167–169, Jul. 2001.

[40] D. Patranabis, *Sensors and transducers*. Prentice-Hall of India, 2004.

[41] J. Jiang, T. Liu, K. Liu, S. Wang, J. Yin, B. Zhao, J. Zhang, L. Song, P. Zhao, F. Wu, and X. Zhang, "Development of optical fiber sensing instrument for aviation and aerospace application," 2013, vol. 9044, p. 90440K.

[42] P. Sobolčiak, A. Tanvir, A. Popelka, J. Moffat, K. A. Mahmoud, and I. Krupa, "The preparation, properties and applications of electrospun co-polyamide 6,12 membranes modified by cellulose nanocrystals," *Mater. Des.*, vol. 132, pp. 314–323, 2017.

[43] S. H. Kim, D. B. Asay, and M. T. Dugger, "Nanotribology and MEMS," *Nano Today*, vol. 2, no. 5, pp. 22–29, Oct. 2007.

[44] N.-C. Tsai and C.-Y. Sue, "Review of MEMS-based drug delivery and dosing systems," *Sensors Actuators A Phys.*, vol. 134, no. 2, pp. 555–564, Mar. 2007.

[45] P. M. Ajayan, O. Stephan, C. Colliex, and D. Trauth, "Aligned Carbon Nanotube Arrays Formed by Cutting a Polymer Resin--Nanotube Composite," *Science (80-. ).*, vol. 265, no. 5176, pp. 1212–1214, Aug. 1994.

[46] Y.-L. Zhao and J. F. Stoddart, "Noncovalent Functionalization of Single-Walled Carbon Nanotubes," *Acc. Chem. Res.*, vol. 42, no. 8, pp. 1161–1171, Aug. 2009.

[47] J. Jang, J. Bae, and S.-H. Yoon, "A study on the effect of surface treatment of

carbon nanotubes for liquid crystalline epoxide–carbon nanotube composites," *J. Mater. Chem.*, vol. 13, no. 4, pp. 676–681, Mar. 2003.

[48] B. Safadi, R. Andrews, and E. A. Grulke, "Multiwalled carbon nanotube polymer composites: Synthesis and characterization of thin films," *J. Appl. Polym. Sci.*, vol. 84, no. 14, pp. 2660–2669, Jun. 2002.

[49] Xiaoyi Gong, * Jun Liu, Suresh Baskaran, and Roger D. Voise, and J. S. Young, "Surfactant-Assisted Processing of Carbon Nanotube/Polymer Composites," 2000.

[50] Rahul Sen, Bin Zhao, Daniel Perea, Mikhail E. Itkis, Hui Hu, James Love, and Elena Bekyarova, and R. C. Haddon*, "Preparation of Single-Walled Carbon Nanotube Reinforced Polystyrene and Polyurethane Nanofibers and Membranes by Electrospinning," 2004.

[51] S. Cui, R. Canet, A. Derre, M. Couzi, and P. Delhaes, "Characterization of multiwall carbon nanotubes and influence of surfactant in the nanocomposite processing," *Carbon N. Y.*, vol. 41, no. 4, pp. 797–809, Jan. 2003.

[52] F. Du, J. E. Fischer, and K. I. Winey, "Coagulation method for preparing single-walled carbon nanotube/poly(methyl methacrylate) composites and their modulus, electrical conductivity, and thermal stability," *J. Polym. Sci. Part B Polym. Phys.*, vol. 41, no. 24, pp. 3333–3338, Dec. 2003.

[53] * Rodney Andrews, David Jacques, and Dali Qian, and T. Rantell, "Multiwall Carbon Nanotubes: Synthesis and Application," 2002.

[54] B. I. Yakobson, C. J. Brabec, and J. Bernholc, "Nanomechanics of Carbon Tubes: Instabilities beyond Linear Response," *Phys. Rev. Lett.*, vol. 76, no. 14, pp. 2511–2514, Apr. 1996.

[55] A.J.Burggraaf, “Chapter 2 Important characteristics of inorganic membranes,” *Membr. Sci. Technol.*, vol. 4, pp. 21–34, Jan. 1996.

[56] P. Pandey and R. S. Chauhan, “Membranes for gas separation,” *Prog. Polym. Sci.*, vol. 26, no. 6, pp. 853–893, Aug. 2001.

[57] M. Padaki, R. Surya Murali, M. S. Abdullah, N. Misdan, A. Moslehyani, M. A. Kassim, N. Hilal, and A. F. Ismail, “Membrane technology enhancement in oil–water separation. A review,” *Desalination*, vol. 357, pp. 197–207, Feb. 2015.

[58] S. S. Madaeni and E. Salehi, “Adsorption of cations on nanofiltration membrane: Separation mechanism, isotherm confirmation and thermodynamic analysis,” *Chem. Eng. J.*, vol. 150, no. 1, pp. 114–121, Jul. 2009.

[59] S. P. Adiga, C. Jin, L. A. Curtiss, N. A. Monteiro-Riviere, and R. J. Narayan, “Nanoporous membranes for medical and biological applications,” *Wiley Interdiscip. Rev. Nanomedicine Nanobiotechnology*, vol. 1, no. 5, pp. 568–581, Sep. 2009.

[60] Y. S. Lin, I. Kumakiri, B. N. Nair, and H. Alsyouri, “MICROPOROUS INORGANIC MEMBRANES,” *Sep. Purif. Methods*, vol. 31, no. 2, pp. 229–379, Jan. 2002.

[61] A. F. Ismail and L. I. B. David, “A review on the latest development of carbon membranes for gas separation,” *J. Memb. Sci.*, vol. 193, no. 1, pp. 1–18, Oct. 2001.

[62] X. Cheng, F. Pan, M. Wang, W. Li, Y. Song, G. Liu, H. Yang, B. Gao, H. Wu, and Z. Jiang, “Hybrid membranes for pervaporation separations,” *J. Memb. Sci.*, vol. 541, pp. 329–346, Nov. 2017.

[63] J. R. Werber, C. O. Osuji, and M. Elimelech, “Materials for next-generation desalination and water purification membranes,” *Nat. Rev. Mater.*, vol. 1, no. 5, p. 16018,

May 2016.

[64] T. Tsuru, “INORGANIC POROUS MEMBRANES FOR LIQUID PHASE SEPARATION,” *Sep. Purif. Methods*, vol. 30, no. 2, pp. 191–220, Jul. 2001.

[65] A. Javaid, “Membranes for solubility-based gas separation applications,” *Chem. Eng. J.*, vol. 112, no. 1–3, pp. 219–226, Sep. 2005.

[66] M. Cheryan and N. Rajagopalan, “Membrane processing of oily streams. Wastewater treatment and waste reduction,” *J. Memb. Sci.*, vol. 151, no. 1, pp. 13–28, Dec. 1998.

[67] L. Feng, Z. Zhang, Z. Mai, Y. Ma, B. Liu, L. Jiang, and D. Zhu, “A Super-Hydrophobic and Super-Oleophilic Coating Mesh Film for the Separation of Oil and Water,” *Angew. Chemie*, vol. 116, no. 15, pp. 2046–2048, Apr. 2004.

[68] B. Hu and K. Scott, “Influence of membrane material and corrugation and process conditions on emulsion microfiltration,” *J. Memb. Sci.*, vol. 294, no. 1–2, pp. 30–39, May 2007.

[69] E. U. Kulawardana and D. C. Neckers, “Photoresponsive oil sorbers,” *J. Polym. Sci. Part A Polym. Chem.*, vol. 48, no. 1, pp. 55–62, Jan. 2010.

[70] B. Su, Y. Tian, and L. Jiang, “Bioinspired Interfaces with Superwettability: From Materials to Chemistry,” *J. Am. Chem. Soc.*, vol. 138, no. 6, pp. 1727–1748, Feb. 2016.

[71] Z. Xue, S. Wang, L. Lin, L. Chen, M. Liu, L. Feng, and L. Jiang, “A Novel Superhydrophilic and Underwater Superoleophobic Hydrogel-Coated Mesh for Oil/Water Separation,” *Adv. Mater.*, vol. 23, no. 37, pp. 4270–4273, Oct. 2011.

[72] A. K. Kota, Y. Li, J. M. Mabry, and A. Tuteja, “Hierarchically Structured Superoleophobic Surfaces with Ultralow Contact Angle Hysteresis,” *Adv. Mater.*, vol. 24,

no. 43, pp. 5838–5843, Nov. 2012.

[73] J. Li, L. Yan, W. Li, J. Li, F. Zha, and Z. Lei, “Superhydrophilic–underwater superoleophobic ZnO-based coated mesh for highly efficient oil and water separation,” *Mater. Lett.*, vol. 153, pp. 62–65, Aug. 2015.

[74] W. Zhang, Y. Cao, N. Liu, Y. Chen, and L. Feng, “A novel solution-controlled hydrogel coated mesh for oil/water separation based on monolayer electrostatic self-assembly,” *RSC Adv.*, vol. 4, no. 93, pp. 51404–51410, Oct. 2014.

[75] T. Darmanin and F. Guittard, “Enhancement of the Superoleophobic Properties of Fluorinated PEDOP Using Polar Glycol Spacers,” *J. Phys. Chem. C*, vol. 118, no. 46, pp. 26912–26920, Nov. 2014.

[76] P.-C. Chen and Z.-K. Xu, “Mineral-Coated Polymer Membranes with Superhydrophilicity and Underwater Superoleophobicity for Effective Oil/Water Separation,” *Sci. Rep.*, vol. 3, no. 1, p. 2776, Dec. 2013.

[77] Z. Xu, Y. Zhao, H. Wang, X. Wang, and T. Lin, “A Superamphiphobic Coating with an Ammonia-Triggered Transition to Superhydrophilic and Superoleophobic for Oil-Water Separation,” *Angew. Chemie Int. Ed.*, vol. 54, no. 15, pp. 4527–4530, Apr. 2015.

[78] K. Liao, X.-Y. Ye, P.-C. Chen, and Z.-K. Xu, “Biomineralized polypropylene/$CaCO_3$ composite nonwoven meshes for oil/water separation,” *J. Appl. Polym. Sci.*, vol. 131, no. 4, p. n/a-n/a, Feb. 2014.

[79] P.-C. Chen and Z.-K. Xu, “Mineral-Coated Polymer Membranes with Superhydrophilicity and Underwater Superoleophobicity for Effective Oil/Water Separation,” *Sci. Rep.*, vol. 3, no. 1, p. 2776, Dec. 2013.

[80] Z. Xue, Y. Cao, N. Liu, L. Feng, and L. Jiang, “Special wettable materials for oil/water separation,” *J. Mater. Chem. A*, vol. 2, no. 8, pp. 2445–2460, Jan. 2014.

[81] R. N. Wenzel, “RESISTANCE OF SOLID SURFACES TO WETTING BY WATER,” *Ind. Eng. Chem.*, vol. 28, no. 8, pp. 988–994, Aug. 1936.

[82] A. B. D. Cassie and S. Baxter, “Wettability of porous surfaces,” *Trans. Faraday Soc.*, vol. 40, no. 0, p. 546, Jan. 1944.

[83] G. Viswanadam and G. G. Chase, “Water–diesel secondary dispersion separation using superhydrophobic tubes of nanofibers,” *Sep. Purif. Technol.*, vol. 104, pp. 81–88, Feb. 2013.

[84] W. Zhang, Z. Shi, F. Zhang, X. Liu, J. Jin, and L. Jiang, “Superhydrophobic and Superoleophilic PVDF Membranes for Effective Separation of Water-in-Oil Emulsions with High Flux,” *Adv. Mater.*, vol. 25, no. 14, pp. 2071–2076, Apr. 2013.

[85] M. H. Tai, P. Gao, B. Y. L. Tan, D. D. Sun, and J. O. Leckie, “Highly Efficient and Flexible Electrospun Carbon–Silica Nanofibrous Membrane for Ultrafast Gravity-Driven Oil–Water Separation,” *ACS Appl. Mater. Interfaces*, vol. 6, no. 12, pp. 9393–9401, Jun. 2014.

[86] C. H. J. M. W. Maad, S.K Samal, Z.C Liu, R. Xiong, S.C.D Smedt, B. Bhush, Q. Zhang, “No Title,” *Sci.*, vol. 537, no. 1, pp. 128–139, 2017.

[87] R. Gopal, S. Kaur, Z. Ma, C. Chan, S. Ramakrishna, and T. Matsuura, “Electrospun nanofibrous filtration membrane,” *J. Memb. Sci.*, vol. 281, no. 1–2, pp. 581–586, Sep. 2006.

[88] L. T. (Simon) Choong, Y.-M. Lin, and G. C. Rutledge, “Separation of oil-in-water emulsions using electrospun fiber membranes and modeling of the fouling mechanism,”

*J. Memb. Sci.*, vol. 486, pp. 229–238, Jul. 2015.

[89] K. Yoon, K. Kim, X. Wang, D. Fang, B. S. Hsiao, and B. Chu, "High flux ultrafiltration membranes based on electrospun nanofibrous PAN scaffolds and chitosan coating," *Polymer (Guildf).*, vol. 47, no. 7, pp. 2434–2441, Mar. 2006.

[90] M. Obaid, N. A. M. Barakat, O. A. Fadali, M. Motlak, A. A. Almajid, and K. A. Khalil, "Effective and reusable oil/water separation membranes based on modified polysulfone electrospun nanofiber mats," *Chem. Eng. J.*, vol. 259, pp. 449–456, Jan. 2015.

[91] Xuefen Wang, Xuming Chen, Kyunghwan Yoon, Dufei Fang, * and Benjamin S. Hsiao, and B. Chu*, "High Flux Filtration Medium Based on Nanofibrous Substrate with Hydrophilic Nanocomposite Coating," 2005.

[92] X. Wang, K. Zhang, Y. Yang, L. Wang, Z. Zhou, M. Zhu, B. S. Hsiao, and B. Chu, "Development of hydrophilic barrier layer on nanofibrous substrate as composite membrane via a facile route," *J. Memb. Sci.*, vol. 356, no. 1–2, pp. 110–116, Jul. 2010.

[93] Y. Li, W. Xiao, K. Xiao, L. Berti, J. Luo, H. P. Tseng, G. Fung, and K. S. Lam, "Well-Defined, Reversible Boronate Crosslinked Nanocarriers for Targeted Drug Delivery in Response to Acidic pH Values and *cis* -Diols," *Angew. Chemie Int. Ed.*, vol. 51, no. 12, pp. 2864–2869, Mar. 2012.

[94] B. Wang, W. Liang, Z. Guo, and W. Liu, "Biomimetic super-lyophobic and super-lyophilic materials applied for oil/water separation: a new strategy beyond nature," *Chem. Soc. Rev.*, vol. 44, no. 1, pp. 336–361, Dec. 2015.

[95] B. Xue, L. Gao, Y. Hou, Z. Liu, and L. Jiang, "Temperature Controlled Water/Oil Wettability of a Surface Fabricated by a Block Copolymer: Application as a Dual

Water/Oil On-Off Switch," *Adv. Mater.*, vol. 25, no. 2, pp. 273–277, Jan. 2013.

[96] G. Ju, M. Cheng, and F. Shi, "A pH-responsive smart surface for the continuous separation of oil/water/oil ternary mixtures," *NPG Asia Mater.*, vol. 6, no. 7, pp. e111–e111, Jul. 2014.

[97] Z. Cheng, J. Wang, H. Lai, Y. Du, R. Hou, C. Li, N. Zhang, and K. Sun, "pH-Controllable On-Demand Oil/Water Separation on the Switchable Superhydrophobic/Superhydrophilic and Underwater Low-Adhesive Superoleophobic Copper Mesh Film," *Langmuir*, vol. 31, no. 4, pp. 1393–1399, Feb. 2015.

[98] G. Kwon, A. K. Kota, Y. Li, A. Sohani, J. M. Mabry, and A. Tuteja, "On-Demand Separation of Oil-Water Mixtures," *Adv. Mater.*, vol. 24, no. 27, pp. 3666–3671, Jul. 2012.

[99] D. Tian, X. Zhang, Y. Tian, Y. Wu, X. Wang, J. Zhai, and L. Jiang, "Photo-induced water–oil separation based on switchable superhydrophobicity–superhydrophilicity and underwater superoleophobicity of the aligned ZnO nanorod array-coated mesh films," *J. Mater. Chem.*, vol. 22, no. 37, p. 19652, Aug. 2012.

[100] H. Che, M. Huo, L. Peng, T. Fang, N. Liu, L. Feng, Y. Wei, and J. Yuan, "$CO_2$-Responsive Nanofibrous Membranes with Switchable Oil/Water Wettability," *Angew. Chemie*, vol. 127, no. 31, pp. 9062–9066, Jul. 2015.

[101] J.-J. Li, Y.-N. Zhou, and Z.-H. Luo, "Smart Fiber Membrane for pH-Induced Oil/Water Separation," *ACS Appl. Mater. Interfaces*, vol. 7, no. 35, pp. 19643–19650, Sep. 2015.

[102] B. Liu, H. Zhou, S. Zhou, H. Zhang, A.-C. Feng, C. Jian, J. Hu, W. Gao, and J. Yuan, "Synthesis and Self-Assembly of $CO_2$–Temperature Dual Stimuli-Responsive

Triblock Copolymers," *Macromolecules*, vol. 47, no. 9, pp. 2938–2946, May 2014.

[103] Z. Guo, Y. Feng, S. He, M. Qu, H. Chen, H. Liu, Y. Wu, and Y. Wang, "$CO_2$-Responsive 'Smart' Single-Walled Carbon Nanotubes," *Adv. Mater.*, vol. 25, no. 4, pp. 584–590, Jan. 2013.

[104] H. Wang, H. Zhou, H. Niu, J. Zhang, Y. Du, and T. Lin, "Dual-Layer Superamphiphobic/Superhydrophobic-Oleophilic Nanofibrous Membranes with Unidirectional Oil-Transport Ability and Strengthened Oil-Water Separation Performance," *Adv. Mater. Interfaces*, vol. 2, no. 4, p. 1400506, Mar. 2015.

[105] R. Crites and G. Tchobanoglous, *Small and decentralized wastewater management systems*. 1998.

[106] B. Van der Bruggen, M. Mänttäri, and M. Nyström, "Drawbacks of applying nanofiltration and how to avoid them: A review," *Sep. Purif. Technol.*, vol. 63, no. 2, pp. 251–263, Oct. 2008.

[107] J. Liu, L. Yu, and Y. Zhang, "Fabrication and characterization of positively charged hybrid ultrafiltration and nanofiltration membranes via the in-situ exfoliation of Mg/Al hydrotalcite," *Desalination*, vol. 335, no. 1, pp. 78–86, Feb. 2014.

[108] X. Fan, Y. Dong, Y. Su, X. Zhao, Y. Li, J. Liu, and Z. Jiang, "Improved performance of composite nanofiltration membranes by adding calcium chloride in aqueous phase during interfacial polymerization process," *J. Memb. Sci.*, vol. 452, pp. 90–96, Feb. 2014.

[109] F. Attiogbe, M. Glover-Amengor, and K. Nyadziehe, "Correlating biochemical and chemical oxygen demand of effluents – A case study of selected industries in Kumasi, Ghana," *West African J. Appl. Ecol.*, vol. 11, no. 1, Sep. 2009.

[110] G. Liu, J. Shen, Q. Liu, G. Liu, J. Xiong, J. Yang, and W. Jin, “Ultrathin two-dimensional MXene membrane for pervaporation desalination,” *J. Memb. Sci.*, vol. 548, pp. 548–558, Feb. 2018.

[111] L. Guo, X. Wang, Z. Y. Leong, R. Mo, L. Sun, and H. Y. Yang, “Ar plasma modification of 2D MXene Ti3C2Tx nanosheets for efficient capacitive desalination,” *FlatChem*, vol. 8, pp. 17–24, Mar. 2018.

[112] G. A. Gebreslase, “Review on Membranes for the Filtration of Aqueous Based Solution: Oil in Water Emulsion,” 2018.

[113] B. Anasori, M. R. Lukatskaya, and Y. Gogotsi, “2D metal carbides and nitrides (MXenes) for energy storage,” *Nat. Rev. Mater.*, vol. 2, no. 2, p. 16098, Feb. 2017.

[114] N. Nady, M. C. R. Franssen, H. Zuilhof, M. S. M. Eldin, R. Boom, and K. Schroën, “Modification methods for poly(arylsulfone) membranes: A mini-review focusing on surface modification,” *Desalination*, vol. 275, no. 1–3, pp. 1–9, Jul. 2011.

[115] Y. Zhu, W. Xie, F. Zhang, T. Xing, and J. Jin, “Superhydrophilic In-Situ-Cross-Linked Zwitterionic Polyelectrolyte/PVDF-Blend Membrane for Highly Efficient Oil/Water Emulsion Separation,” *ACS Appl. Mater. Interfaces*, vol. 9, no. 11, pp. 9603–9613, Mar. 2017.

[116] Y. Liao, M. Tian, and R. Wang, “A high-performance and robust membrane with switchable super-wettability for oil/water separation under ultralow pressure,” *J. Memb. Sci.*, vol. 543, pp. 123–132, Dec. 2017.

[117] Q. F. Alsalhy, “Hollow fiber ultrafiltration membranes prepared from blends of poly (vinyl chloride) and polystyrene,” *Desalination*, vol. 294, pp. 44–52, May 2012.

[118] M. Padaki, R. Surya Murali, M. S. Abdullah, N. Misdan, A. Moslehyani, M. A.

Kassim, N. Hilal, and A. F. Ismail, “Membrane technology enhancement in oil–water separation. A review,” *Desalination*, vol. 357, pp. 197–207, Feb. 2015.

[119] D. da S. Biron, M. Zeni, C. P. Bergmann, V. dos Santos, D. da S. Biron, M. Zeni, C. P. Bergmann, and V. dos Santos, “Analysis of Composite Membranes in the Separation of Emulsions Sunflower oil/water,” *Mater. Res.*, vol. 20, no. 3, pp. 843–852, May 2017.

[120] Y.-B. Zhou, X.-Y. Tang, X.-M. Hu, S. Fritschi, and J. Lu, “Emulsified oily wastewater treatment using a hybrid-modified resin and activated carbon system,” *Sep. Purif. Technol.*, vol. 63, no. 2, pp. 400–406, Oct. 2008.

[121] X. Zhu, A. Dudchenko, X. Gu, and D. Jassby, “Surfactant-stabilized oil separation from water using ultrafiltration and nanofiltration,” *J. Memb. Sci.*, vol. 529, pp. 159–169, May 2017.

[122] X. S. Yi, S. L. Yu, W. X. Shi, N. Sun, L. M. Jin, S. Wang, B. Zhang, C. Ma, and L. P. Sun, “The influence of important factors on ultrafiltration of oil/water emulsion using PVDF membrane modified by nano-sized TiO2/Al2O3,” *Desalination*, vol. 281, pp. 179–184, Oct. 2011.

[123] B. A. Madaan V, chanana A, Kataria MK, “Emulsion Technology and Recent Trends in Emulsion Applications,” *Int Res J Pharm*, vol. 5, pp. 533–542, 2014.

[124] T. Darvishzadeh, V. V. Tarabara, and N. V. Priezjev, “Oil droplet behavior at a pore entrance in the presence of crossflow: Implications for microfiltration of oil–water dispersions,” *J. Memb. Sci.*, vol. 447, pp. 442–451, Nov. 2013.

[125] J.-H. Zuo, P. Cheng, X.-F. Chen, X. Yan, Y.-J. Guo, and W.-Z. Lang, “Ultrahigh flux of polydopamine-coated PVDF membranes quenched in air via thermally induced

phase separation for oil/water emulsion separation," *Sep. Purif. Technol.*, vol. 192, pp. 348–359, Feb. 2018.

[126] X. Huang, W. Wang, Y. Liu, H. Wang, Z. Zhang, W. Fan, and L. Li, "Treatment of oily waste water by PVP grafted PVDF ultrafiltration membranes," *Chem. Eng. J.*, vol. 273, pp. 421–429, Aug. 2015.

[127] B. Saini, M. K. Sinha, and S. K. Dash, "Mitigation of HA, BSA and oil/water emulsion fouling of PVDF Ultrafiltration Membranes by SiO2-g-PEGMA nanoparticles," *J. Water Process Eng.*, Apr. 2018.

[128] T. Ahmad, C. Guria, and A. Mandal, "Optimal synthesis and operation of low-cost polyvinyl chloride/bentonite ultrafiltration membranes for the purification of oilfield produced water," *J. Memb. Sci.*, vol. 564, pp. 859–877, Oct. 2018.

[129] GRIFFIN and W. C., "Calculation of HLB Values of Non-ionic Surfactants," *J. Soc. Cosmet. Chem.*, vol. 5, pp. 249–256, 1954.

[130] M. C. S. Gomes, P. A. Arroyo, and N. C. Pereira, "Influence of oil quality on biodiesel purification by ultrafiltration," *J. Memb. Sci.*, vol. 496, pp. 242–249, Dec. 2015.

[131] H.-H. Tseng, J.-C. Wu, Y.-C. Lin, and G.-L. Zhuang, "Superoleophilic and superhydrophobic carbon membranes for high quantity and quality separation of trace water-in-oil emulsions," *J. Memb. Sci.*, vol. 559, pp. 148–158, Aug. 2018.

[132] H. P. Ngang, A. L. Ahmad, S. C. Low, and B. S. Ooi, "Adsorption-desorption study of oil emulsion towards thermo-responsive PVDF/SiO2-PNIPAM composite membrane," *J. Environ. Chem. Eng.*, vol. 5, no. 5, pp. 4471–4482, Oct. 2017.

[133] B. Chakrabarty, A. K. Ghoshal, and M. K. Purkait, "Ultrafiltration of stable oil-in-water emulsion by polysulfone membrane," *J. Memb. Sci.*, vol. 325, no. 1, pp. 427–437,

Nov. 2008.

[134] “GE MW Ultrafiltration (UF) Membrane,... - YMMWSP475 | Sterlitech.” [Online]. Available: https://www.sterlitech.com/ultrafiltration-uf-membrane-ymmwsp475.html#. [Accessed: 13-Dec-2018].

[135] S. Sun, C. Liao, A. M. Hafez, H. Zhu, and S. Wu, “Two-dimensional MXenes for energy storage,” *Chem. Eng. J.*, vol. 338, no. October 2017, pp. 27–45, 2018.